Zincohögbomite and gahnite in a diaspore-bearing metabauxite from eastern Samos (Greece) : mineral chemistry, element partitioning and reaction relations

Autor(en): **Feenstra, Anne**

Objekttyp: **Article**

Zeitschrift: **Schweizerische mineralogische und petrographische Mitteilungen = Bulletin suisse de minéralogie et pétrographie**

Band (Jahr): **77 (1997)**

Heft 1

PDF erstellt am: **19.09.2024**

Persistenter Link: https://doi.org/10.5169/seals-58470

SCHWEIZ. MINERAL. PETROGR. MITT. 77, 73–93, 1997

Zincohögbomite and gahnite in a diaspore-bearing metabauxite from eastern Samos (Greece): mineral chemistry, element partitioning and reaction relations

by *Anne Feenstra*[1]

Abstract

Zincohögbomite, ranging in X_{Zn} [= Zn/(Zn + Fe^{2+} + Mg + Ni + Co)] from 0.64 to 0.80, is a minor constituent of low-grade polymetamorphic diaspore-bearing metabauxites from E-Samos. Textural relations indicate that högbomite, which particularly occurs in the lower contact zone between diasporite and marble, is a late phase mainly forming from gahnite and rutile during greenschist-grade metamorphism that followed early Alpine high-P metamorphism. Other phases in the zincohögbomite-bearing samples are Fe-rich chloritoid (X_{Zn} < 0.01), Zn-dominated staurolite (X_{Zn} = 0.59–0.77), calcite, (Ti)hematite, white Na–K–Ca micas, tourmaline and rare Ni-rich chlorite. Three white micas occur in most samples, with margarite and paragonite typically interlayered on a submicron-scale. Chloritoid is widespread in the Samos diasporites, whereas Zn-staurolite is only a local constituent.

The Samos zincohögbomite contains up to 4.6 wt% NiO and 1.3 wt% CoO. Electron microprobe data indicate that both low-Ti (5.9–7.3 wt% TiO_2) and high-Ti (9.6–10.5 wt% TiO_2) högbomites occur, sometimes within the same thin section. This variation in Ti may be related to different hexagonal (nH) and/or rhombohedral högbomite (nR) structure types, which however could not be determined by XRD methods due to the minor amount of högbomite present. The associated gahnite is generally rich in Zn (X_{Zn} > 0.86) and contains up to 1.17 wt% NiO and 1.56 wt% CoO. Element partitioning between högbomite and gahnite is systematic; högbomite invariably has higher Ni/Co, Fe/Zn and Fe/Mg than gahnite. Högbomite and gahnite display a much stronger Fe–Zn and Fe–Mg fractionation in the low-grade Samos rocks than documented for occurrences in amphibolite- to granulite-grade rocks. Textures, chemical data and analysis of phase-relations suggest that the Samos zincohögbomite formed by the reaction:

gahnite + rutile + (Ti)-hematite + diaspore = zincohögbomite + H_2O + O_2

or in hematite-free samples by a continuous reaction of the type:

gahnite + rutile + Fe-rich chloritoid + calcite = zincohögbomite + Fe-poorer chloritoid + margarite + H_2O + CO_2.

Pressure conditions of högbomite growth are poorly constrained but muscovite-paragonite thermometry applied on closely associated micas results in temperatures of 270–320 °C. The occurrence of margarite, and possibly primary kaolinite, is also consistent with temperatures around 300 °C (at 5 kbar), provided that the metamorphic fluid was very water-rich. The unusual Zn–Ni–Co rich bulk compositions that allowed the formation of Zn-dominated högbomite, spinel and staurolite at such low metamorphic grades probably arise from pronounced pre-metamorphic trace element enrichment at the footwall of the karstbauxite.

Keywords: zincohögbomite, gahnite, Fe–Zn–Mg–Ni–Co partitioning, diaspore metabauxite, P-T conditions, mineral chemistry, Samos, Greece.

Introduction

Högbomite, a complex Fe–Mg–Ti–Al oxide, typically occurs as a minor or accessory constituent in medium to high-grade metamorphosed Al-rich or mafic rocks, as well as in Fe–Ti oxide ore deposits (see review of PETERSEN et al., 1989). In many of these rocks, textural observations suggest that högbomite is not a typical peak metamorphic mineral but formed during retrogradation and/or a late (waning) stage of a polymetamorphic cycle (e.g., COOLEN, 1981; RAMMLMAIR et al., 1988; PETERSEN et al., 1989; GREW et al., 1990; VISSER et al., 1992, and references therein). In virtually all cases, högbomite is closely associated with (Fe, Mg,Zn)Al_2O_4 and/or Fe_3O_4 spinel. Textural evi-

[1] Institut für Petrologie, Geozentrum Universität Wien, Althanstrasse 14, A-1090 Wien, Austria.

dence, such as högbomite overgrowing and enclosing the spinel, suggests that hogbömite mainly formed at the expense of spinel, while Ti may have been supplied by rutile or ilmenite in the rocks. In cases, where högbomite is genetically associated with magnetite, högbomite growth may be related to retrograde oxidation-exsolution of an initially homogeneous Al–Mg–Zn containing titanomagnetite (e.g., ANGUS and MIDDLETON, 1985; GREW et al., 1990). Fe–Ti oxides associated

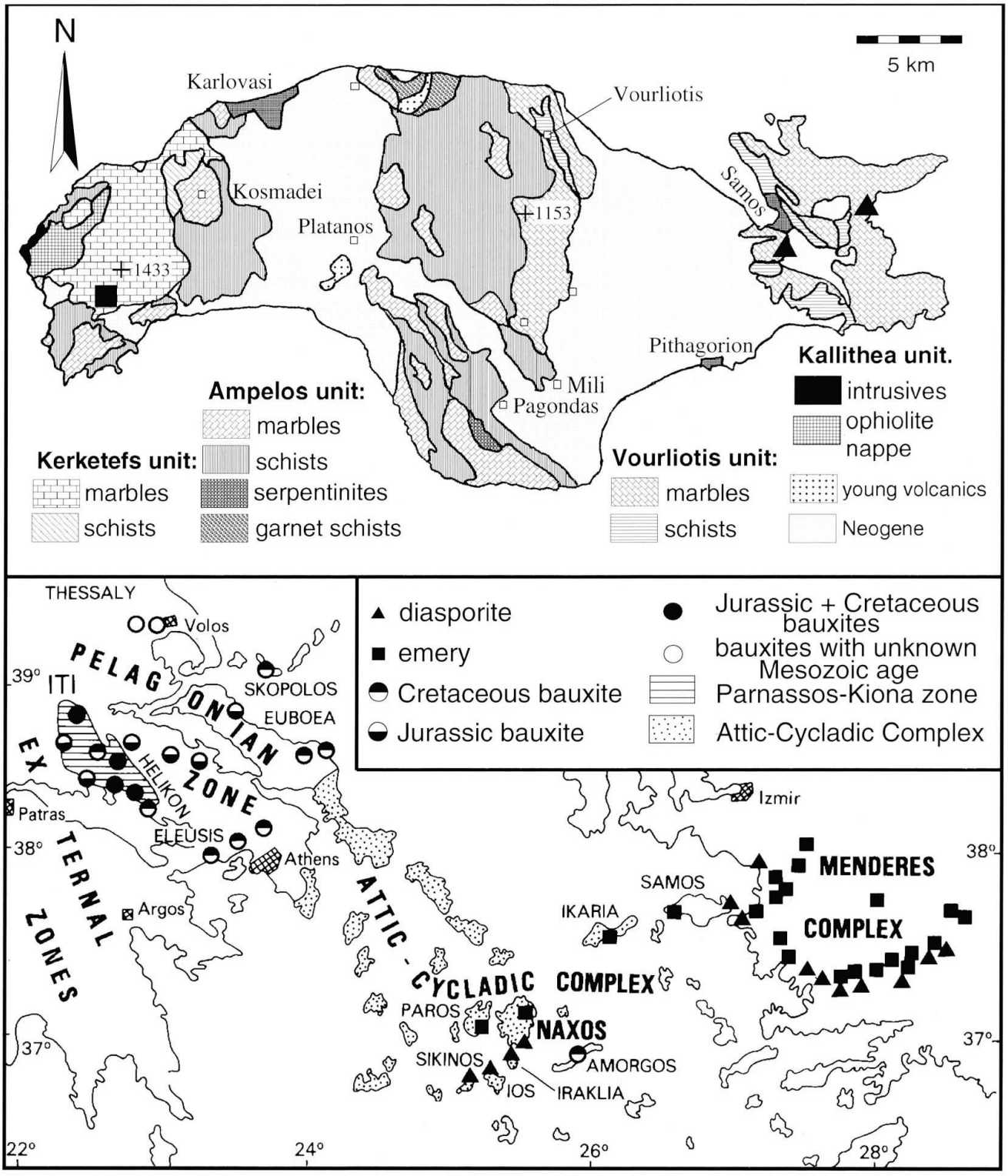

Fig. 1 Distribution of metabauxites and Mesozoic karstbauxites in the central Aegean region (FEENSTRA, 1985). The studied metabauxite is indicated by the triangle at the eastern coast of Samos (≈ 4 km E of Samos town). The geological map of Samos (upper diagram) is simplified and slightly modified after THEODOROPOLOUS (1979) and PAPANIKOLAOU (1979).

with högbomite commonly monitor oxidizing conditions, indicating that high f_{O_2} could be an important factor in högbomite formation.

The complex crystal stucture of högbomite can be modelled as consisting of alternating layers with cubic spinel-like ($R^{2+}Al_2O_4$) and hexagonal nolanite-like ($TiAl_4O_8$) structures. Different stacking sequences, in which cubic layers dominate, result in various structural types with hexagonal (nH) or rhombohedral (nR) lattices (McKIE, 1963; GATEHOUSE and GREY,1982; PETERSEN et al., 1989; SCHMETZER and BERGER, 1990). The partial similarity of the högbomite structure with that of spinel also explains the frequently observed epitaxic relationship between both phases, with högbomite (0001) faces orientated parallel to the (111) faces of the spinel host (e.g., PETERSEN et al., 1989; SCHMETZER and BERGER, 1990; YALÇIN et al., 1993).

Whereas most högbomite is an Fe–Mg–Ti–Al solid solution, varieties containing considerable amounts of zinc are also known (e.g., WILSON, 1977; COOLEN, 1981; SPRY, 1982; ANGUS and MIDDLETON, 1985; FEENSTRA, 1985; PETERSEN et al., 1989; SPRY and PETERSEN, 1989; GREW et al., 1990). In greenschist-grade metabauxites along the southern margin of the Menderes Complex in SW-Turkey (see Fig. 1), YALÇIN et al. (1993) documented högbomite with X_{Zn} between 0.42 and 0.60. For such Zn-dominant högbomite from the Menderes and Samos metabauxites, OCKENGA et al. (in prep.) proposed the name zincohögbomite (IMA no. 94-016; approved as a new mineral by the IMA Commission on New Minerals and Mineral Names).

The present paper describes a comparable occurrence of högbomite stabilized at low metamorphic grade by high Zn content in diaspore-bearing metabauxitic rocks from E-Samos (Fig. 1). Like in the Menderes metabauxites, the Samos zincohögbomite is genetically related to gahnite. The studied Samos samples were all collected from the same diasporite lens but vary considerably in mineral assemblage and composition. This allowed to investigate the mineral chemistry of zincohögbomite and gahnite, and the element partitioning between both oxides over a large, unusually Zn-rich, compositional range at a single low metamorphic grade.

Geological setting

The island of Samos occupies a transitional position between the Attic-Cycladic-Metamorphic Complex (ACMC) in the Aegean Sea and the Menderes-Complex in SW-Turkey (Fig. 1). Both complexes are largely composed of late Paleozoic-Mesozoic (vulcano-)sedimentary sequences metamorphosed during Alpine times (e.g., DÜRR, 1975, 1986; SCHLIESTEDT et al., 1987; OKRUSCH and BRÖCKER, 1990). Thick Mesozoic carbonate units are common in the ACMC and the cover of the Menderes Complex. They locally contain metamorphosed karstbauxite deposits (see Fig. 1), testifying of periods of (local) emersion and concomitant chemical weathering, interrupting the Mesozoic neritic carbonate sedimentation. The most extensive metabauxite deposits are found on Naxos (FEENSTRA, 1985, 1996) and along the western and southern margins of the Menderes Complex (ÖNAY, 1949; YALÇIN, 1987). In both regions, numerous (2–5 meter thick) metabauxite lenses, which are usually confined to specific stratigraphic horizons, occur in thick-bedded calcitic marbles. Depending on metamorphic grade, the metabauxites are either diaspore-bearing (diasporites) or at the higher grades corundum-bearing (emeries). FEENSTRA and MAKSIMOVIC (1985a) inferred a Jurassic stratigraphic age for the Naxos metabauxites from geochemical comparison with Mesozoic karstbauxites in Central Greece (Fig. 1). A similar stratigraphic age may also hold for the Menderes metabauxites (YALÇIN, 1987).

Due to late vertical movements, the metamorphic rock sequence of Samos is dissected in western, central and eastern crystalline blocks, separated by grabens filled with Neogene sediments and volcanics (Fig. 1). Whereas THEODOROPOLOUS (1979) assumed that Samos is composed of a more less continuous sequence of metamorphic rocks (in the extreme west covered by the ophiolite nappe of Kallithea), PAPANIKOLAOU (1979) proposed a nappe-like structure for the metamorphic complex, including three main tectonic units (Fig. 1).

The lowest tectonic unit is the Kerketefs unit, which occupies the mountainous region of western Samos. It mainly consists of > 1000 m thick, partly dolomitic, marbles. A small corundum-bearing metabauxite lens occurs in the marbles of the southern slope of Kerketefs Mountain (MPOSKOS, 1978).

The Kerketefs unit is overlain by the Ampelos unit, a highly variable sequence of alternating schists and marbles, locally containing intercalations of metabasic rocks (blueschists and greenschists), ultramafics (mainly serpentinites) and metagabbros (OKRUSCH et al., 1984; MPOSKOS et al., 1990; CHEN, 1992; FEENSTRA and PETRAKAKIS, in prep.). The Ampelos unit occurs around Kerketefs Mountain and constitutes the main part of the central crystalline area.

The Vourliotis unit, buiding up the eastern margin of the central crystalline area and the entire eastern crystalline area, is the structurally highest metamorphic nappe of Samos. The unit is composed of prominant upper and lower marble horizons (both several hundreds meters thick) and intercalated pelitic to psammitic schists. Like the Ampelos unit, it is characterized by local occurrences of metabasic, ultrabasic und metagabbroic rocks. In eastern Samos, several diasporite lenses occur in the upper marble horizon of the Vourliotis unit (DE LAPPERENT, 1937; MPOSKOS, 1978).

Like most metamorphic rocks of the ACMC, those of Samos evidence a polymetamorphic evolution. Although unconfirmed by geochronological work, an early high-P blueschist facies event, particularly affecting the Ampelos and Vourliotes units (OKRUSCH et al., 1984; CHEN, 1992; FEENSTRA and PETRAKAKIS, in prep.), can probably be correlated with the early Alpine high-P (M1) event in the ACMC, which ended at 40–50 Ma (e.g., SCHLIESTEDT et al., 1987; WYBRANS and MCDOUGALL, 1988; OKRUSCH and BRÖCKER, 1990; FEENSTRA, 1996). The high-P mineral assemblages of Samos, which include glaucophane in basic, gabbroic and pelitic compositions, are in varying degrees overprinted by greenschist-facies assemblages (OKRUSCH et al., 1984; CHEN, 1992; FEENSTRA and PETRAKAKIS, in prep.). As a medium-P greenschist-facies event is of regional significance in the ACMC, it is tempting to correlate the medium-P overprint with the M2-event in the ACMC, dated at 20–25 Ma (e.g., SCHLIESTEDT et al., 1987; WYBRANS and MCDOUGALL, 1988; OKRUSCH and BRÖCKER, 1990).

Studying metapelitic and metabasic rocks of northern, central and eastern Samos, CHEN (1992) derived for the high-P event temperatures of 510–540 °C in northern Samos (for the garnet schists in Fig. 1), ≈ 500 °C in central Samos (Ampelos unit) and ≈ 470 °C in the eastern part of the island (Vourliotis unit). In all regions pressures were estimated to be ≈ 12 kbar. Conditions during the medium-P metamorphism, a transistional event related to the uplift of the blueschist facies rocks, are poorly constrained. CHEN (1992) arrived at P–T conditions of 460–490 °C and ≈ 7 kbar, without discernible regional variations in the studied area.

Metamorphic conditions for the western crystalline area (Kerketefs and Ampelos units) are only roughly known. Lithologies containing mineral assemblages suitable for precise P-T determinations are scarce (MPOSKOS and PERDIKATZIS, 1981; FEENSTRA and PETRAKAKIS, in prep.). Unlike the diasporites of eastern Samos (Vourliotis unit), the small metabauxite lens in the Kerketefs marbles contains corundum (MPOSKOS, 1978), indicating somewhat higher conditions for bauxite metamorphism than in eastern Samos. It is unclear, however, whether the corundum formed during the high- or medium-P event.

Petrography of the Samos metabauxites

The Samos metabauxites were previously studied by DE LAPPERENT (1937) and MPOSKOS (1978). Both researchers concentrated their investigations on the main mass of the metabauxites, which in E-Samos is characterized by the paragenesis diaspore + Ti-hematite + rutile + chloritoid and in W-Samos, where metamorphic conditions slightly exceeded the diaspore-corundum dehydration reaction, by corundum + diaspore + ilmenohematite/ilmenite + rutile + chloritoid. Minor amounts of muscovite, paragonite and gahnite are also present in the deposits of both regions. Högbomite is a rare mineral in the bulk of the Samos metabauxites. Nevertheless, DE LAPPERENT (1937) already described a yellowish to brown anisotropic mineral, predominantly overgrowing the octahedral faces of gahnite, which he called "taosite" but actually was högbomite.

In the present study (högbomite + gahnite)-bearing samples, all collected from a diasporite lens located along the eastern coast of Samos (≈ 4 kilometers E of Samos town; see Fig. 1), were selected for detailed electron microprobe (EMP) investigations. Most samples are from the lower contact of the diasporite lens with calcitic marbles of the Vourliotis unit. The diasporite, which has partly been mined as bauxite ore during the beginning of the century, is exposed over a length of about 80 meters with a maximum thickness of 4–5 meters.

On the scale of a thin section, the samples consist of silicate- and oxide-rich domains or layers in a matrix predominantly composed of calcite and minor white mica. The typical zincian mineral assemblages observed in the samples include gahnite + zincohögbomite, gahnite + zincohögbomite + chloritoid and gahnite + zincohögbomite + Zn-staurolite (Tab. 1; Fig. 2). Trace amounts of Ni-rich chlorite occur in some samples but chlorite always seems to be a late phase. Minerals present in all samples are diaspore, rutile, calcite, white micas and tourmaline. Traces of hematite, commonly altered to Fe-hydroxide, also occur in most samples.

Two types of gahnite can texturally be distinguished. The first (older) type, which is present in all samples, forms 50–400 μm large crystals that are colourless to light blue. It typically occurs as

Tab. 1 Mineralogy of studied Samos metabauxites.

Sample No.	Dsp	Gh	Ho	Cld	St	Chl	Pg	Ms	Mrg	Cal	Hem	Rt	Tur	Other*
AFS1C	X	O	O	O			X	X		X	O[a]	O	O	
SA22A1	O	O	O	X		O	O[b]	X	O[c]	X	O[a]	O	O	Ap, Kln
SA22A2	O	O	O				O[b]	X	O[c]	X	O[a]	O	O	Mnz
SA22A32	O	X	O	X[d]	O[d]		O[b]	X	O[c]	X	X[e]	O	O	Kln
SA22B	O	X	O		O	O	X[b]	X	O[c]	X		O	O	
SA22B1	O	X	O		O	O	X[b]	O	O[c]	X		O	O	
SA99	O	O	O		X		X	X		X	O[a]	O	O	Zrn

Mineral abbreviations: Gh = gahnite; Ho = högbomite; other mineral abbreviations used are after Kretz (1983); X = major mineral; O = minor mineral; * minerals grouped under other occur in trace amounts

[a] allered to Fe-hydroxide

[b] paragonite lamellae intimitely intergrown with margarite and/or muscovite and too thin for EMP analysis

[c] margarite flakes intimitely intergrown with paragonite and too thin for EMP analysis

[d] chloritoid and staurolite not in contact but occurring 1–2 mm apart

[e] hematite contains 11–13 mole% ilmenite in solid solution

dispersed equidimensional grains (Fig. 2). The second (younger) gahnite type forms smaller blue-coulored crystals (< 100 μm in size), which are texturally related to partial breakdown of staurolite. It tends to be richer in Co (up to 1.56 wt% CoO) than the larger first-generation gahnite crystals (particularly their cores). The first-type gahnite contains abundant inclusions of calcite, rutile, diaspore, tourmaline, muscovite and paragonite (Fig. 2C). Particularly the cores of the larger grains are crowded with such inclusions. Chloritoid and staurolite are fairly rare as inclusions in gahnite; chloritoid was observed in some first-type gahnite grains of sample SA22A1 (Fig. 2C) and relictic staurolite in second-type gahnite grains of samples SA22A32 and SA22B1.

Zincohögbomite is always closely associated with gahnite. The yellow to brown pleochroitic mineral typically forms epitaxial rims on and (platy) intergrowths with gahnite (Fig. 2). In some samples discrete idiomorphic högbomite crystals also occur (Fig. 2B). Similar preferential growth of högbomite on the octahedral faces of gahnite crystals was documented by YALÇIN et al. (1993) in the metabauxites of the Menderes Complex. This textural relationship, which results from common structural properties of close oxygen packing in both minerals (e.g., GATEHOUSE and GREY, 1982; SCHMETZER and BERGER, 1990; YALÇIN et al., 1993), suggests that högbomite predominantly grew at the expense of gahnite. The overall textural evidence, such as högbomite forming at the expense of both generations of gahnite and the lack of högbomite inclusions in any mineral, indicates that Samos zincohögbomite formed late during the polymetamorphic history of the rocks.

Chloritoid is by far the dominant Fe–Mg–Al silicate in greenschist-grade metabauxitic rocks (FEENSTRA, 1985: YALÇIN, 1987). In the studied rocks, it forms lath-shaped crystals of variable size (Fig. 2C). Polysynthetic twinning and pleochroism are diagnostic optical features. Rutile, Ti-hematite, diaspore, muscovite and paragonite are common inclusions in chloritoid.

Zn-staurolite forms subidiomorphic prismatic porphyroblasts (up to 0.4 mm long) that display light-bluish to colourless pleochroism. The bluish colour may arise from its minor CoO content (< 0.55 wt%). Staurolite crystals contain inclusions of calcite, rutile, Ti-hematite, diaspore, white mica and, more rarely, gahnite. The inclusions are particularly abundant in the central parts of the grains, giving the mineral a cloudy appearance in thin sections. Staurolite is in variable degrees replaced by the second-generation gahnite, white mica and, less commonly, zincohögbomite and Ni-rich chlorite. In the Samos rocks, staurolite and chloritoid were not observed in mutual contact, as is the case in the Naxos and Ios metabauxites (FEENSTRA, 1985; FEENSTRA and OCKENGA, in prep.). Thin section SA22A32 (Tab. 1) contains staurolite and chloritoid but they occur ≈ 2 mm apart.

In all samples, variable amounts of muscovite and paragonite are present as dispersed flakes in the calcite matrix. Both micas are most abundant in domains rich in högbomite, staurolite or chloritoid. The white K- and Na-micas are commonly interlayered on a (sub)micron scale, complicating analysis by EMP (FEENSTRA, 1996). Using BSE-imaging on the EMP, incipient growth of margarite was observed within paragonite-rich areas in most samples (Tab. 1). The margarite and paragonite lamellae typically alternate on a scale beyond the resolution of the EMP.

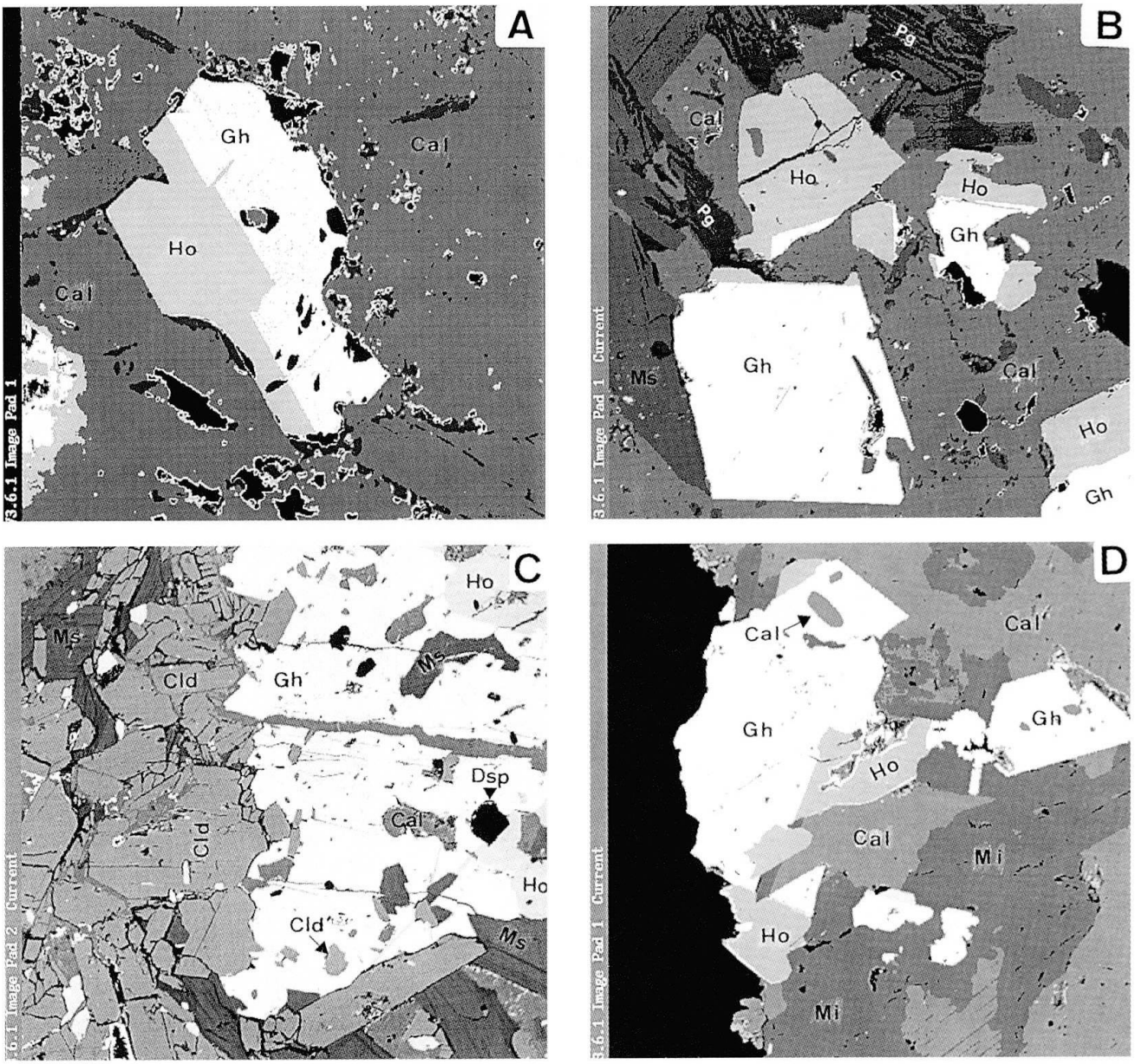

Fig. 2 Back-scaterred electron micrographs showing textural relations between zincohögbomite (Ho) and gahnite (Gh) in diasporites from E-Samos. (A) Sample AFS1C: Epitaxial intergrowth of zincohögbomite and gahnite. Matrix consists of (poorly polished) calcite (Cal). Width of picture is 230 μm. (B) Sample SA22A1: Idiomorphic gahnite and zincohögbomite in matrix consisting of calcite, muscovite (Ms) and paragonite (Pg). Width of picture is 320 μm. (C) Composite gahnite-högbomite grain in chloritoid-rich part of sample SA22A1. Gahnite contains inclusions of chloritoid (Cld), diaspore (Dsp), calcite and muscovite. Width of picture is 360 μm. (D) Sample SA22A2: Aggregate of zincohögbomite and gahnite surrounded by white mica (Mi) and calcite. The mica is mainly paragonite with submicron-size intercalations of margarite and muscovite, which are not visible at the used magnification. Width of picture is 230 μm.

Mineral chemistry

ANALYTICAL METHOD

Minerals were analyzed by electron microprobe using wavelength-dispersive analysis techniques. Operation conditions were 15 kV accelerating potential, 20 nA beam current and a beam diameter of 1–2 μm. Peak counting times were 15–20 seconds for major and 20–60 seconds for minor elements; backgrounds were counted for 8–20 seconds. Standards used included the following synthetic or natural minerals and metals: garnets (Fe, Mn, Si, Al); ilmenites (Fe, Mn, Ti); feldspars (Si, Al, Ca, Na, K); spinel (Mg, Al); gahnite (Zn, Al): sphalerite (Zn); eskolaite (Cr); barite (Ba); $SrCO_3$ (Sr); metallic V, Zn, Ni and Co. The raw spectrometer data were corrected with the "PAP" program

(POUCHOU and PICHOIR, 1985). The quality and reproducibility of the analyses were monitored by including well-known standards in the analysis sessions. Average gahnite and högbomite compositions and associated 1 σ standard deviations are listed in tables 2 and 3.

GAHNITE

The EMP work showed that cores of the (large) first-generation gahnite crystals tend to be highest in Zn with some analyses approaching $ZnAl_2O_4$ endmember (cf. Fig. 3a). In the staurolite-bearing samples, the marginal parts of the first-type gahnite grains compositionally match the second-generation gahnite. The latter displays little chemical variation within individual crystals but grains separated by more than a few mm may differ in composition in the thin sections. Because the present study is focused on the reaction relations and element distribution between zincohögbomite and gahnite, and the former only appears to be in equilibrium with the second-type gahnite and the rims of the first-type gahnite, core compositions of the first-generation gahnite, which maybe relics of

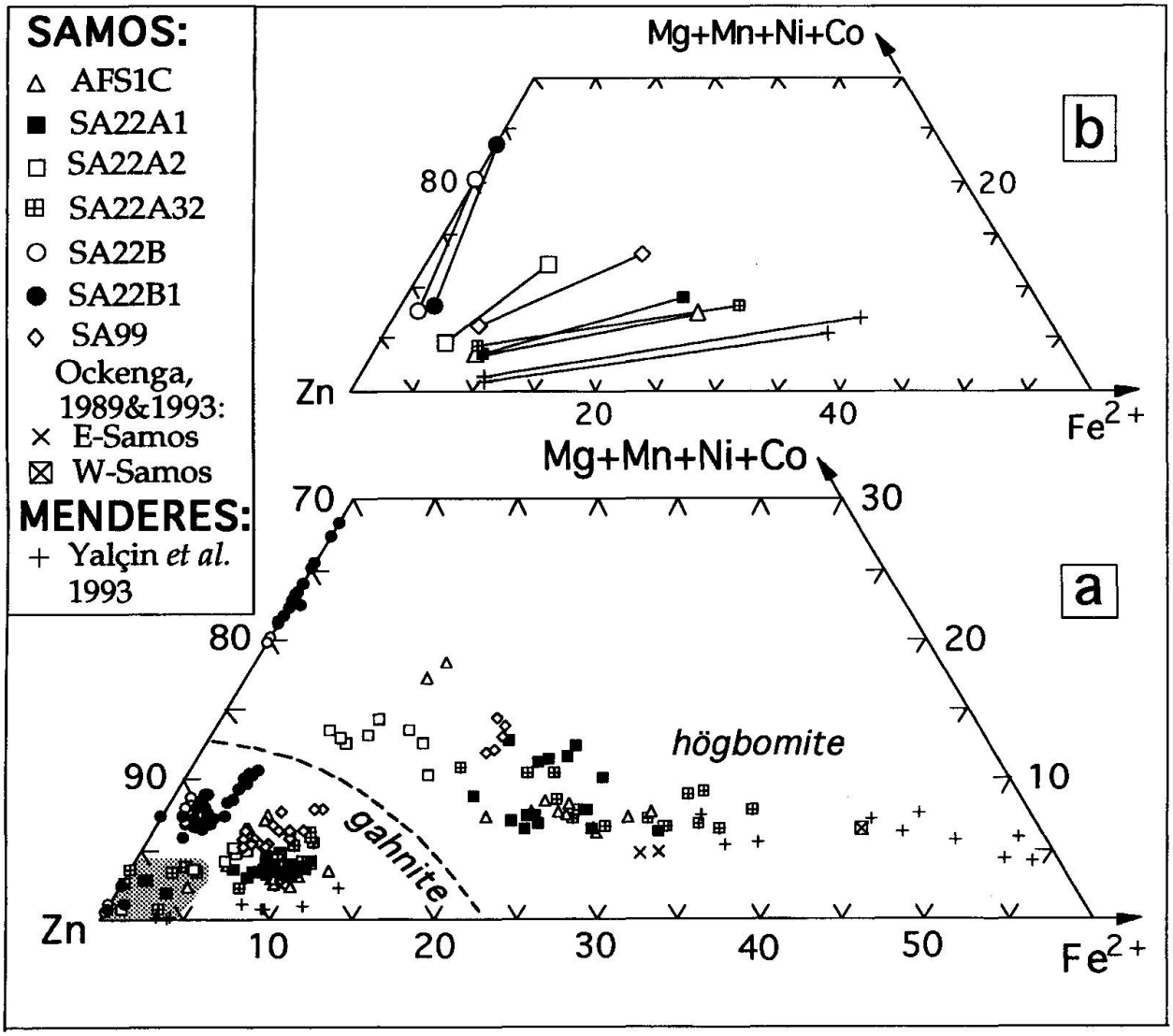

Fig. 3 Compositional variation of gahnite and zincohögbomite in the studied Samos diasporites depicted in a molar Zn–Fe^{2+}–(Mg + Ni + Co + Mn) diagram. For comparison, gahnite and högbomite data reported for the Menderes (YALÇIN et al., 1993) and Samos metabauxites (OCKENGA; 1989 and in YALÇIN et al., 1993) are also shown.
(a) Individual spot analyses. Dashed line separates gahnite and högbomite analyses. The most zincian Samos spinel compositions plotting in the shaded field in the lower left corner are predominantly from the cores of large first-generation gahnite grains (see text). (b) Average compositions of closely associated gahnite and högbomite connected by tie-lines.

Tab. 2 Gahnite compositions[@].

	AFS1C (17)*	SA22A1 (24)	SA22A2 (6)	SA22A32 (21)	SA22B (9)	SA22B1 (27)	SA99 (18)
SiO_2	0.04 (3)*	0.03 (2)	0.04 (1)	0.03 (2)	0.04 (2)	0.05 (4)	0.04 (3)
TiO_2	0.06 (11)	0.02 (2)	0.05 (3)	0.08 (14)	0.02 (2)	0.11 (14)	0.11 (15)
Al_2O_3	56.07 (54)	55.94 (22)	56.29 (32)	55.37 (52)	56.76 (37)	56.59 (41)	56.42 (25)
Cr_2O_3	0.42 (68)	0.32 (30)	0.53 (37)	0.20 (23)	0.36 (30)	0.39 (32)	0.22 (30)
V_2O_3	0.19 (22)	b.d.	b.d.	b.d.	0.13 (22)	0.10 (20)	0.18 (23)
FeO**	3.38 (96)	3.81 (38)	2.21 (20)	3.24 (83)	1.00 (11)	1.29 (17)	3.10 (40)
MgO	0.32 (5)	0.32 (2)	0.44 (5)	0.29 (10)	0.43 (4)	0.39 (7)	0.22 (6)
MnO	0.05 (4)	0.07 (2)	0.05 (3)	0.08 (4)	0.04 (2)	0.04 (4)	0.06 (4)
ZnO	39.38 (68)	39.23 (89)	40.71 (80)	38.51 (117)	41.65 (50)	40.46 (142)	38.88 (118)
NiO	0.30 (23)	0.21 (9)	0.31 (7)	0.49 (27)	0.90 (23)	1.17 (49)	0.52 (27)
CoO	0.65 (53)	0.60 (10)	0.73 (9)	0.61 (20)	1.53 (11)	1.50 (20)	1.56 (26)
Total	100.85 (58)	100.55 (77)	101.35 (69)	98.90 (57)	102.88 (66)	102.09 (113)	101.31 (91)
Formulae on the basis of 4 oxygens and 3 cations							
Si	0.001 (1)	0.001 (1)	0.001 (0)	0.001 (1)	0.001 (1)	0.002 (1)	0.001 (1)
Ti	0.001 (2)	0.000 (1)	0.001 (1)	0.002 (3)	0.001 (0)	0.002 (3)	0.002 (4)
Al	1.985 (13)	1.986 (11)	1.985 (13)	1.997 (12)	1.976 (12)	1.982 (18)	1.989 (14)
Cr	0.010 (16)	0.008 (7)	0.013 (9)	0.005 (6)	0.008 (7)	0.009 (7)	0.005 (7)
V^{3+}	0.005 (5)	–	–	–	0.003 (5)	0.002 (5)	0.004 (5)
Fe^{3+}	0.002 (4)	0.007 (7)	0.002 (4)	0.002 (5)	0.009 (6)	0.004 (6)	0.003 (6)
$SumR^{3+}$	2.005 (8)	2.002 (9)	2.001 (4)	2.007 (7)	1.998 (1)	2.002 (7)	2.006 (10)
Fe^{2+}	0.083 (23)	0.089 (11)	0.054 (8)	0.081 (22)	0.016 (4)	0.028 (10)	0.074 (11)
Mg	0.014 (2)	0.014 (1)	0.020 (2)	0.013 (4)	0.019 (2)	0.017 (3)	0.010 (2)
Mn	0.001 (1)	0.002 (1)	0.001 (1)	0.002 (1)	0.001 (1)	0.001 (1)	0.002 (1)
Zn	0.874 (17)	0.873 (17)	0.899 (15)	0.870 (29)	0.909 (7)	0.888 (26)	0.859 (23)
Ni	0.007 (6)	0.005 (2)	0.008 (2)	0.012 (7)	0.021 (6)	0.028 (12)	0.013 (7)
Co	0.016 (13)	0.015 (2)	0.018 (2)	0.015 (5)	0.036 (3)	0.036 (5)	0.037 (6)
$SumR^{2+}$	0.995 (10)	0.998 (9)	0.999 (4)	0.993 (7)	1.002 (1)	0.998 (7)	0.994 (10)
Mole fractions							
XFe^{2+}	0.083 (22)	0.089 (12)	0.054 (8)	0.081 (22)	0.016 (4)	0.028 (10)	0.075 (12)
XMg	0.014 (2)	0.014 (1)	0.020 (2)	0.013 (5)	0.019 (2)	0.017 (3)	0.010 (2)
XMn	0.001 (1)	0.002 (1)	0.001 (1)	0.002 (1)	0.001 (1)	0.001 (1)	0.002 (1)
XZn	0.878 (19)	0.875 (12)	0.901 (13)	0.876 (28)	0.907 (7)	0.890 (21)	0.864 (18)
XNi	0.007 (6)	0.005 (2)	0.008 (2)	0.012 (7)	0.021 (6)	0.028 (12)	0.013 (7)
XCo	0.016 (13)	0.015 (2)	0.018 (2)	0.015 (5)	0.036 (3)	0.036 (5)	0.038 (6)

[@] Average compositions are based on analyses of second-type gahnite and marginal parts of first-type grains (see text).

* The number of analyses and 1σ standard deviation in terms of the last digit(s) are given in parentheses. b.d. = below detection limit; ** total iron is expressed as FeO.

the (prograde?) high-P metamorphic stage, were excluded in calculating the average compositions given in table 2.

The spinel stoichiometry calculated on the basis of 4 oxygens and 3 cations suggests negligible ferric iron (Tab. 2). Spinel is generally rich in zinc, containing more than 86 mole% $ZnAl_2O_4$ component (Tab. 2; Fig. 3). Its average $FeAl_2O_4$ component ranges from 1.6 to 8.9 mole%, whereas the $MgAl_2O_4$ component is ≤ 2.0 mole% (Tab. 2). Average $NiAl_2O_4$ and $CoAl_2O_4$ components amount up to 2.8 and 3.8 mole%, respectively. The blue-coloured spinel in the staurolite-bearing samples (SA22B, 22B1 and 99) is richer in Co than the spinel in the chloritoid-containing samples (Fig. 4). The Co may have been inherited from the decomposing staurolite, which contains up to 0.55 wt% CoO. Central portions of large, first-generation spinel crystals dispersed in the matrix usually have the lowest Co (and Ni) content, although some exceptions have been found.

The Samos gahnite belongs to the most zincian spinels reported in the literature (e.g., SANDHAUS and CRAIG, 1986; FROST, 1991). Gahnite analyzed by YALÇIN et al. (1993) from the diasporites of the Menderes Complex compares in $ZnAl_2O_4$ and $MgAl_2O_4$ components with that from Samos but contains only trace amounts of Ni and Co, therefore plotting near the Zn–Fe^{2+} base-line in figure 3.

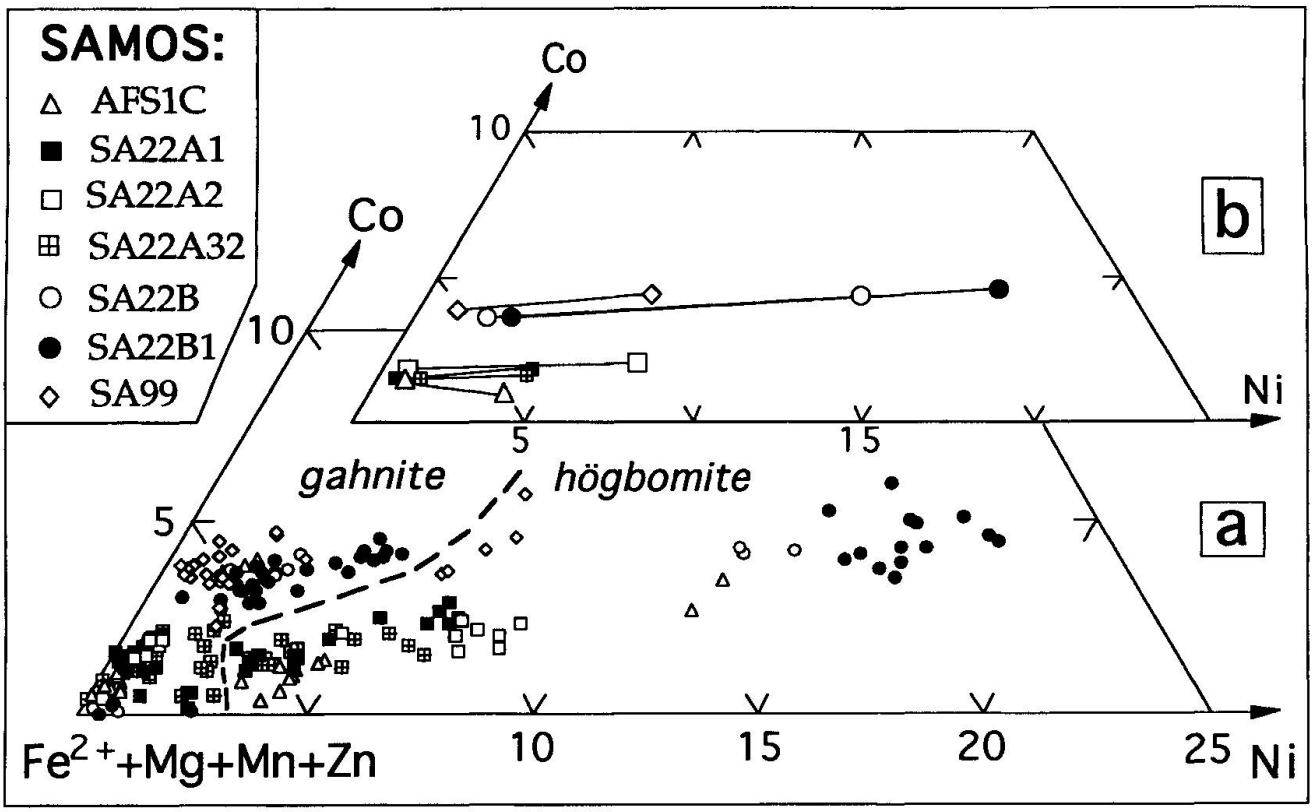

Fig. 4 Compositional variation of Samos gahnite and zincohögbomite in terms of a molar (Fe^{2+} + Mg + Mn + Zn)–Ni–Co diagram. Dashed line in (a) separates gahnite and zincohögbomite analyses. Tie-lines in (b) connect average compositions of closely associated gahnite and högbomite.

ZINCOHÖGBOMITE

All högbomite analyzed in this study contains > 50% Zn endmember, justifying its classification as zincohögbomite (OCKENGA et al., in prep). Furthermore, it is characterized by the presence of variable amounts of Fe, very small amounts of Mg (≤ 0.45 wt% MgO) and significant amounts of Ni and Co (Tab. 3; Figs 3 and 4). The NiO content shows a considerable spread, ranging from 1.27 wt% in sample AFS1C up to 4.57 wt% in sample SA22B1. The CoO content is in the range 0.31–1.28 wt%. The abnormally high SiO_2 content of högbomite in samples SA22A2 and 22B is most likely due to contamination of the EMP analyses with fine-grained silicate inclusions. Hence SiO_2 was ignored in calculating the structural formulae. The analyzed högbomites can roughly be divided in low-Ti (5.6–7.3 wt% TiO_2) and high-Ti (9.6–10.5 wt% TiO_2) types (Tab. 3 and Fig. 5). Oxide totals of the högbomite analyses are below 100% (95.5–98.7 wt%) with total iron expressed as ferrous. This deficit can only partly be explained by high ferric iron and may also be related to the presence of light elements such as H, Li and Be that are not detectable by EMP. Heavy elements known to occur in högbomite (e.g. Sn, Zr) have been sought by WDS element scans but were not detected in significant amounts.

There is no general agreement whether the högbomite structure contains hydroxyl groups or not (see discussions in GREW et al., 1987; PETERSEN et al., 1989; VISSER et al., 1992). Hence no consensus exists how to calculate structural formulae. In addition, the occurrence of various hexagonal (nH) and rhombohedral (nR) structure types (MCKIE, 1963; GATEHOUSE and GREY, 1982; PETERSEN et al., 1989) and apparently highly variable Fe^{3+}/Fe^{2+} ratios (unknown from EMP work) complicate precise understanding of the mineral chemistry of högbomite. ZAKREWSKI (1977) suggested an anhydrous simplified högbomite formula of $R^{2+}_{(8-2x)}Ti_xR^{3+}_{16}O_{32}$, where R^{2+} = Fe^{2+}, Mg, Zn, Ni, Co and R^{3+} = Al, Fe^{3+}, Cr, V^{3+}. This normalization scheme, which yields for x = 1 a formula of $R^{2+}_6TiR^{3+}_{16}O_{32}$, has been widely used since then. GATEHOUSE and GREY (1982) refined the crystal structure of an 8-H type and found an occupancy of 22 cations and an anion composition of (30 O + 2 OH), corresponding to composition $R^{2+}_5TiR^{3+}_{16}O_{30}(OH)_2$.

Structural formulae of the Samos zincohög-

Tab. 3 Högbomite compositions.

Sample	AFS1C (10)[@]	SA22A1 (13)	SA22A2 (8)	SA22A32 (15)	SA22B (3)	SA22B1(16)	SA99 (5)	
SiO_2	0.02 (1)[@]	0.03 (3)	[0.40][a] (24)	0.03 (2)	[0.75][a] (22)	0.12 (5)	0.04 (2)	
TiO_2	5.94 (63)	6.20 (57)	9.62 (28)	5.61 (97)	10.45 (23)	10.14 (59)	7.30 (19)	
Al_2O_3	56.50 (70)	56.18 (58)	58.46 (18)	56.19 (52)	57.92 (52)	56.55 (124)	56.03 (23)	
Cr_2O_3	0.17 (24)	0.21 (22)	0.12 (18)	0.09 (11)	0.17 (12)	0.20 (20)	0.35 (36)	
V_2O_3	0.24 (20)	b.d.	b.d.	b.d.	0.44 (33)	0.12 (17)	0.24 (21)	
FeO[b]	9.85 (55)	9.55 (83)	4.61 (34)	9.58 (124)	2.17 (12)	2.75 (56)	8.11 (36)	
MgO	0.36 (2)	0.33 (2)	0.45 (1)	0.33 (2)	0.40 (2)	0.33 (6)	0.27 (6)	
MnO	0.08 (4)	0.06 (2)	0.05 (3)	0.08 (3)	0.07 (5)	0.06 (3)	0.04 (4)	
ZnO	23.37 (51)	23.17 (88)	21.78 (29)	21.79 (66)	22.02 (64)	22.65 (89)	22.34 (20)	
NiO	1.27 (18)	1.36 (43)	1.93 (32)	1.34 (32)	3.27 (21)	4.57 (67)	1.98 (16)	
CoO	0.31 (11)	0.54 (16)	0.53 (7)	0.50 (10)	1.09 (3)	1.24 (20)	1.28 (27)	
Total	98.11 (76)	97.65 (76)	97.54 (49)	95.54 (60)	98.01 (128)	98.72 (78)	98.00 (40)	
Normalization	32 O*	31 O + 22 cations**	32 O	31 O + 22 cations	32 O	32 O	31 O + 22 cations	32 O	32 O	32 O	31 O + 22 cations
Si	0.00 (0)	0.00 (0)	0.01 (1)	0.01 (1)	0.00	0.01 (1)	0.01 (1)	0.00	0.03 (1)	0.01 (0)	0.01 (0)
Al	15.48 (13)	14.83 (7)	15.44 (17)	14.83 (14)	15.59 (8)	15.75 (20)	15.07 (10)	15.39 (10)	15.10 (22)	15.26 (8)	14.77 (7)
Cr	0.03 (4)	0.03 (4)	0.04 (4)	0.04 (4)	0.02 (3)	0.02 (2)	0.02 (2)	0.03 (2)	0.04 (4)	0.06 (7)	0.06 (6)
V^{3+}	0.05 (4)	0.04 (4)	–	–-	–-	–	–	0.08 (6)	0.02 (3)	0.04 (4)	0.04 (4)
Fe^{3+}	0.44 (14)	1.10 (19)	0.51 (16)	1.03 (21)	0.39 (7)	0.23 (18)	0.98 (28)	0.41 (2)	0.52 (11)	0.61 (8)	0.65 (9)
$SumR^{3+}$	16.00	16.00 (22)	15.99	15.90 (20)	16.00	16.00	16.07 (34)	15.91 (12)	15.71 (19)	15.99	15.53 (6)
Fe^{2+}	1.48 (23)	0.74 (14)	1.36 (23)	0.76 (8)	0.48 (13)	1.68 (42)	0.84 (7)	0.00	0.00	0.95 (3)	0.86 (7)
Mg	0.13 (1)	0.12 (2)	0.12 (1)	0.11 (1)	0.15 (0)	0.12 (1)	0.11 (1)	0.14 (1)	0.11 (2)	0.09 (2)	0.09 (2)
Mn	0.02 (2)	0.01 (1)	0.01 (0)	0.01 (0)	0.01 (1)	0.02 (1)	0.02 (1)	0.01 (1)	0.01 (1)	0.01 (1)	0.01 (1)
Zn	4.01 (10)	3.84 (9)	3.99 (14)	3.83 (13)	3.64 (4)	3.83 (11)	3.66 (12)	3.66 (8)	3.79 (17)	3.81 (3)	3.69 (3)
Ni	0.24 (3)	0.23 (3)	0.26 (8)	0.25 (8)	0.35 (6)	0.26 (6)	0.25 (6)	0.59 (3)	0.83 (12)	0.37 (3)	0.36 (3)
Co	0.06 (2)	0.05 (2)	0.10 (3)	0.10 (3)	0.10 (1)	0.10 (2)	0.09 (2)	0.20 (0)	0.23 (4)	0.24 (5)	0.23 (5)
$SumR^{2+}$	5.93 (22)	5.00 (11)	5.83 (20)	5.05 (10)	4.73 (9)	5.99 (33)	4.97 (17)	4.60 (9)	4.97 (24)	5.47 (7)	5.24 (3)
Ti	1.04 (11)	1.00 (11)	1.09 (10)	1.04 (10)	1.64 (4)	1.00 (17)	0.96 (17)	1.77 (5)	1.73 (9)	1.27 (3)	1.23 (3)
Total cations	22.96 (11)	22.00	22.91 (10)	22.00	22.36 (4)	23.00 (17)	22.00	22.28 (5)	22.41 (9)	22.73 (3)	22.00
Mole fractions											
XFe^{2+}	0.249 (30)	0.147 (26)	0.232 (32)	0.149 (15)	0.101 (26)	0.278 (56)	0.169 (10)	0.000	0.000	0.174 (4)	0.165 (13)
XMg	0.021 (3)	0.024 (3)	0.020 (2)	0.022 (1)	0.032 (1)	0.020 (2)	0.022 (1)	0.029 (1)	0.023 (4)	0.017 (4)	0.017 (4)
XMn	0.003 (1)	0.003 (1)	0.002 (1)	0.002 (1)	0.002 (1)	0.003 (1)	0.003 (1)	0.003 (2)	0.002 (1)	0.002 (1)	0.002 (2)
XZn	0.678 (28)	0.769 (24)	0.685 (30)	0.759 (30)	0.770 (21)	0.641 (47)	0.737 (20)	0.796 (7)	0.763 (20)	0.696 (9)	0.704 (6)
XNi	0.040 (5)	0.046 (6)	0.044 (15)	0.048 (15)	0.074 (12)	0.043 (12)	0.049 (11)	0.129 (7)	0.167 (20)	0.067 (5)	0.068 (6)
XCo	0.010 (3)	0.011 (4)	0.017 (5)	0.019 (6)	0.020 (3)	0.016 (3)	0.018 (4)	0.043 (1)	0.045 (6)	0.043 (9)	0.044 (9)

[@] The number of analyses and 1 σ standard deviation in terms of the last digit(s) are given in parentheses.

[a] SiO_2 values were ignored in calculating structural formulae (see text); b.d. = below detection limit; [b] total iron is expressed as FeO.

* normalized on the basis of 32 O and full occupancy of R^{3+} site (ZAKREWSKI, 1977); ** normalized on the basis of 22 cations and 30 O + 2 OH (GATEHOUSE and GREY, 1982).

bomites calculated according to the anhydrous ZAKREWSKI (1977) formula are listed in table 3. The normalization results in 1.00–1.27 Ti atoms per formulae unit (p.f.u.) for the low-Ti högbomites. For the high-Ti högbomites, Ti is between 1.64–1.77 atoms p.f.u. In the Ti- and Ni-rich (Fe-poor) högbomites of samples SA22B and 22B1 it is impossible, even with all iron expressed as ferric, to fill completely the R^{3+} sites, as is assumed in ZAKREWSKI's model (Tab. 3). Such apparent positive charge deficiency could result from the presence of unanalyzed light cations, so that the applied normalization may be inappropriate for these högbomites. Because the low-Ti högbomites are compositionally close to the $R^{2+}_5TiR^{3+}_{16}O_{30}(OH)_2$ stoichiometry found by GATEHOUSE and GREY (1982) for an 8-H polytype, a normalization on the basis of 22 cations and 31 oxygens (assuming 2 OH) is included for comparison in table 3. The latter results in slightly lower Ti (0.96–1.23 atoms p.f.u.) and in significantly higher Fe^{3+}/Fe^{2+} ratios than the ZAKREWSKI (1977) normalization.

The variation in Ti of the individual högbomite analyses is graphically illustrated in figure 5. Although it may result in overestimated R^{2+}/Ti ratios, total iron is used in the diagram, because calculation of Fe^{3+}/Fe^{2+} ratios from EMP data is highly uncertain without knowledge of OH and vacancy contents of the högbomite (cf. Tab. 3). The diagram of figure 5 suggests that the Samos högbomite varies primarily in composition by way of $(Fe,Ni,Co)_2Ti_{-1}\square_{-1}$ (and possibly $Fe^{3+}_4Ti_{-3}\square_{-1}$) substitution, whereas Zn is fairly constant. The latter may indicate that the associated gahnite essentially buffered the Zn content of högbomite. In figure 5, the low-Ti högbomites plot fairly close to R^{2+}_6Ti and R^{2+}_5Ti stoichiometries. The first composition is obtained by substituting x = 1 in ZAKREWSKI's model, whereas the second one corresponds to that of the 8-H polytype determined by GATEHOUSE and GREY (1982). The high-Ti högbomites plot around $R^{2+}_5Ti_{1.5}$ stoichiometry, obtained by substituting x = 1.5 in ZAKREWSKI's model.

Considerable chemical variation, notably in TiO_2, has been encountered in many EMP studies of högbomite (e.g., PETERSEN et al., 1989; GREW et al., 1990). Such compositional heterogeneity may indicate that the rocks have failed to equilibrate on the scale of a thin section. Alternatively, it may imply that different structural types of högbomite, each characterized by its own chemistry (PETERSEN et al., 1989; VISSER et al., 1992), are present in the samples. Intergrowths of various struc-

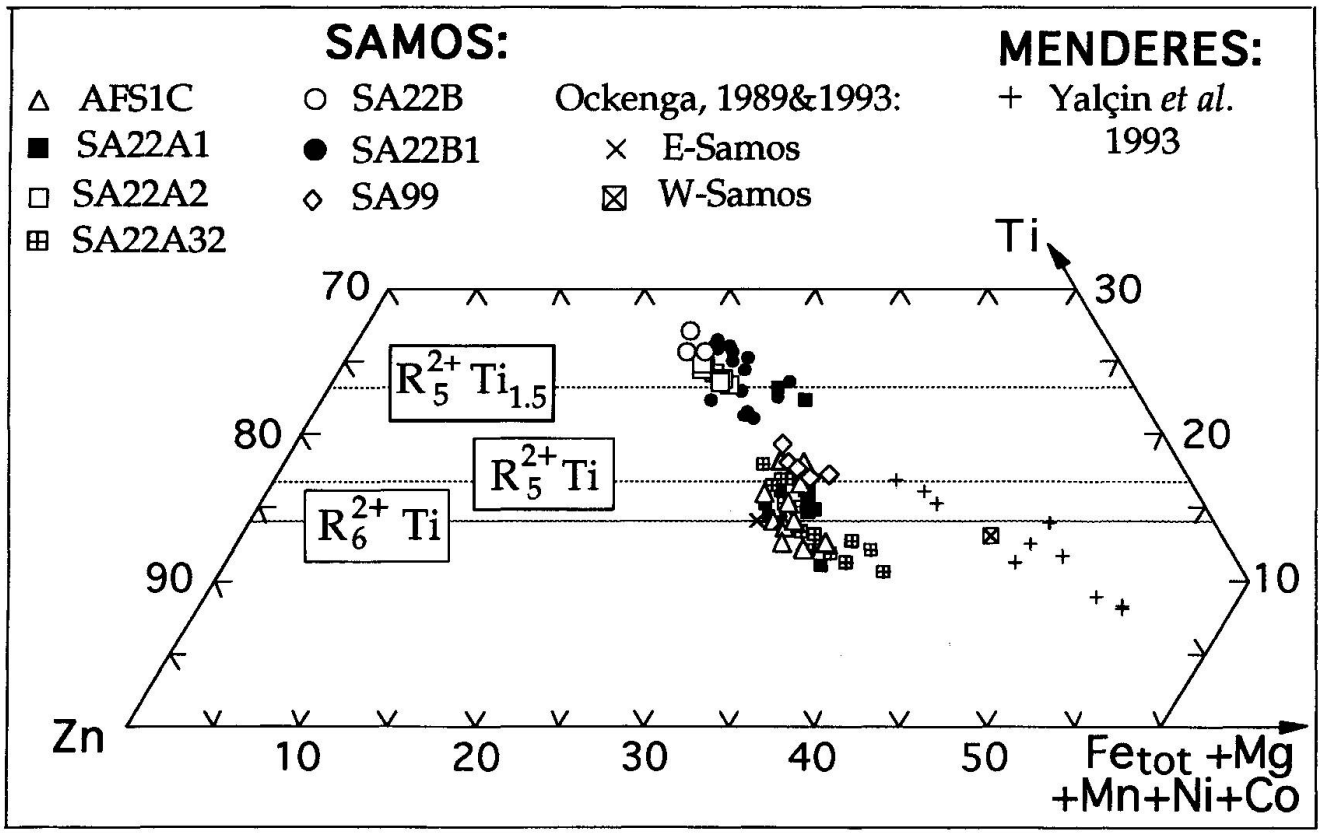

Fig. 5 Compositional variation of Samos and Menderes högbomite in terms of a molar Zn–(Fe_{tot} + Mg + Mn + Co + Ni)-Ti diagram. Dashed lines indicate various theoretical högbomite compositions (see text).

tures on a submicron scale, possibly also with intercalated spinel layers (SCHMETZER and BERGER, 1990), could then explain the variation in högbomite composition within samples. This possibility could be tested by detailed TEM and AEM studies of petrologically well characterized högbomite.

Unfortunately, the crystal structure(s) of the studied zincohögbomite could not be determined, as the minor amounts of högbomite (frequently intergrown with gahnite) hamper separation of enough material for X-ray diffraction studies. OCKENGA et al. (in prep.) determined a 8H structure for a zincohögbomite from the emery deposit of W-Samos. Its chemical composition best matches the low-Ti type of the present study (OCKENGA, personal comm.), making a 8H structure for the latter also plausible.

The studied zincohögbomites contain 21.8–23.4 wt% ZnO, corresponding to 64.1–79.6 mole% $Zn^{2+}_{(8-2x)}Ti_xR^{3+}_6O_{32}$ endmember according to ZAKREWSKI'S normalization (Fig. 3; Tab. 3). They are probably the most Zn-rich ones yet reported, being more zincian than högbomites associated with metamorphosed sulphide deposits (e.g., PETERSEN et al., 1989; SPRY and PETERSEN, 1989). The compositions of the most zincian högbomites from the Menderes metabauxites (from diasporite) match those of the most iron-rich ones of the present study but the majority of the Menderes högbomites (from emery) is poorer in Zn and richer in Fe (YALÇIN et al., 1993; see Fig. 3). This compositional trend is consistent with the observation of YALÇIN et al. (1993) that högbomite will be enriched in Fe and impoverished in Zn (and Ti) with increasing grade in a metabauxitic paragenesis. Chemical data for Samos högbomite reported by OCKENGA (1989; data in YALÇIN et al., 1993) also follow the trend; the two analyses of högbomite from diasporite (E-Samos) compare to those of the present study, while the analysis of högbomite from emery (W-Samos) compares to that of the emery-grade Menderes högbomite (cf. Figs 3 and 5).

Variable amounts of Ni and Co occur in the Samos högbomite (Fig. 4). The highest Ni concentrations are measured in the högbomite of sample SA22B1, containing on average 4.6 wt% NiO (16.7 mole% Ni-högbomite). Nickel is typically present only in trace amounts in högbomite analyses reported in the literature. Högbomite being that rich in Ni as in the Samos samples is unknown to the author. The Samos högbomite contains up to 1.28 wt% CoO (4.5 mole% Co-högbomite). Up to 6.97 wt% CoO was reported by ČECH et al. (1976) for a högbomite from Zambia associated with cobaltoan staurolite.

OTHER MINERALS

The chemistry of the other phases occurring in the samples studied (Tab. 1) is only briefly discussed in the present report. A more complete description will be given in a following paper on Zn-rich mineral assemblages in greenschist-grade Aegean metabauxites that is particularly focused on Zn-rich staurolite and its reaction relations (FEENSTRA and OCKENGA, in prep.).

Compositionally, chloritoid is very similar in the three chloritoid-bearing samples studied. It is composed of 82–83 mole% Fe-, 10–11 mole% Mg-, and 4–5 mole% Mn-endmember. Zn, Ni and Co occur in minor amounts, each constituting < 1.5 mole% of their respective endmembers. The chloritoid is strongly enriched in manganese relative to spinel, högbomite and staurolite, whereas it is very poor in zinc (< 0.27 wt% ZnO) compared to these minerals.

Compared to chloritoid, staurolite is much more variable in composition. Its mineral chemistry is dominated by the Zn-endmember (X_{Zn} = 0.59–0.77). The mole fraction of Fe ranges from 0.07 to 0.28, whereas X_{Mg} and X_{Mn} are less than 0.043 and 0.015, respectively. The Samos staurolite contains up to 1.12 wt% NiO (X_{Ni} = 0.079) and 0.55 wt% CoO (X_{Co} = 0.046).

Diaspore, rutile and calcite occur in all samples and are essentially pure phases. Diaspore contains between 0.2 and 0.7 wt% Fe_2O_3; some abnormally high TiO_2 values (up to 0.7 wt%) are most likely due to incorporation of tiny rutile inclusions. Rutile contains up to 0.6 wt% Cr_2O_3 and 1.3 wt% Fe_2O_3. Calcite typically contains less than 0.4 wt% FeO, 1.6 wt% MgO and 0.1 wt% MnO. Its ZnO content varies between 0.1 and 0.35 wt%. Inclusions of calcite in spinel tend to be richer in MnO (up to 1.5 wt%) and ZnO (up to 1.1 wt%), but as the size of the inclusions is < 20 μm (see e.g., Fig. 2C), the higher Zn content may largely be due to edge effects with the gahnite host during EMP analysis.

Element partitioning between gahnite and högbomite

Högbomite and gahnite, which span a considerable range in Fe–Zn–Mg substitution in the analyzed samples, display a systematic Fe–Zn and Fe–Mg distribution (Fig. 6 b–e), with högbomite always being the more Fe-rich phase. The Ni–Co partitoning between both oxides (Fig. 6a) shows considerable scatter but högbomite generally has a strong preference for Ni (see also Fig. 4). Gahnite and högbomite grains may differ in composi-

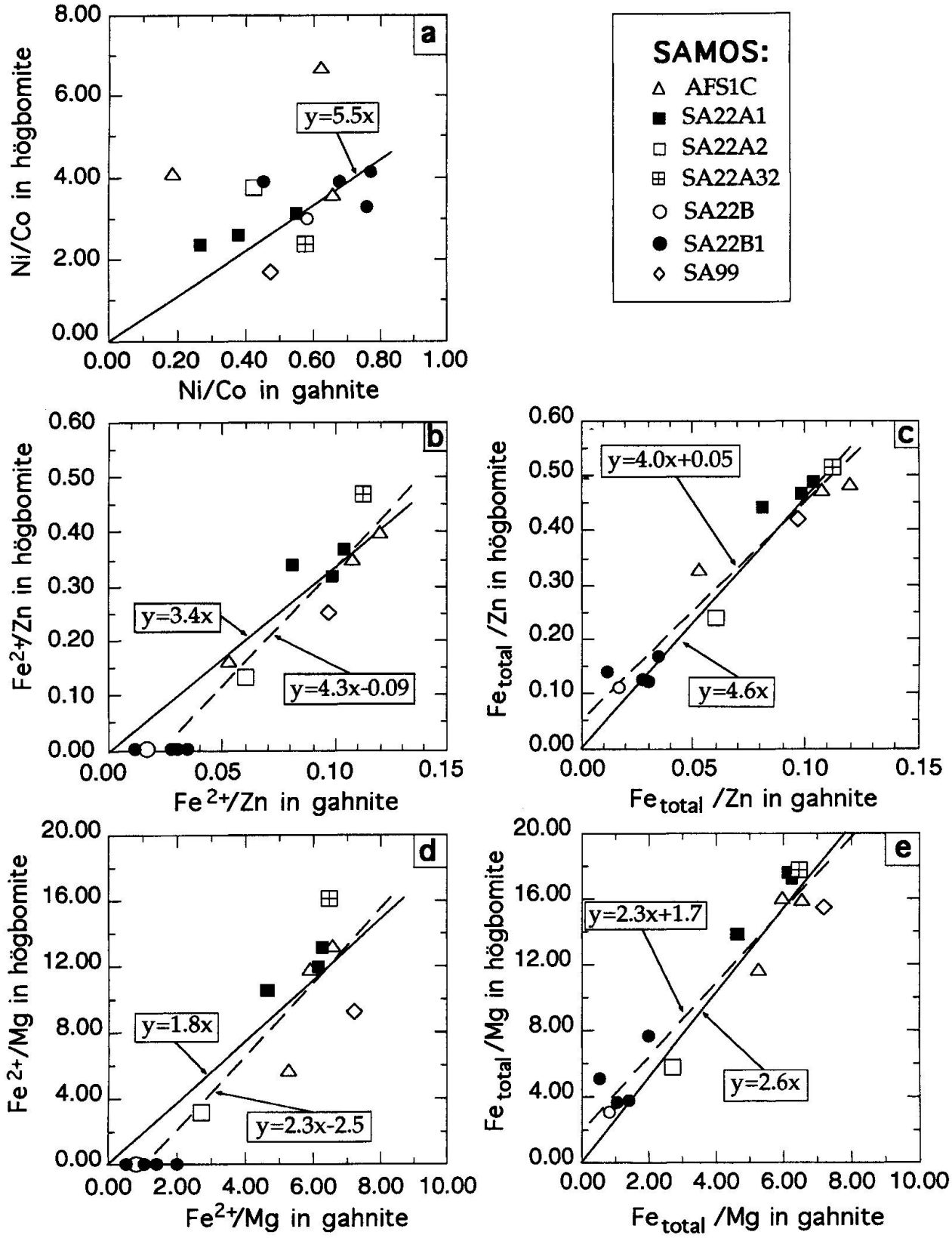

Fig. 6 Element partitioning between gahnite and zincohögbomite in the Samos samples. Plotted symbols represent averages for adjacent gahnite and zincohögbomite. Atomic ratios for zincohögbomite plotted in (b) and (d) are based on structural formulae calculated after ZAKREWSKI (1977). Two least square regression lines for K_D are shown in (b–e), of which the solid one was forced to pass through the origin. In (a) two anomalous data from sample AFS1C were exluded from the regression; in (b) and (d) data plotting at zero values for Fe^{2+}/Zn and Fe^{2+}/Mg in zincohögbomite, respectively, were discarded in the regressions passing through the origin.

tion in various parts of the thin sections; in these cases averages for adjacent gahnite and högbomite in the various domains have been plotted instead of an average for the whole thin section. It should also be noted that thin sections SA22A1, 22A2 and 22A32, which were all cut from a single ≈ 10 · 15 · 25 cm³ large sample, contain compositionally different gahnite and högbomite. Nevertheless, the Fe–Zn–Mg partitioning between both oxides appears regular, demonstrating that, at least on a mm-scale, chemical equilibrium has been attained.

As discussed above, estimation of Fe^{3+}/Fe^{2+} in högbomite from EMP data is highly problematic. Least squares regression of the högbomite-gahnite Fe^{2+}/Zn and Fe^{2+}/Mg distribution data results in regression lines intersecting the y-axis at negative values (dashed lines in Figs 6 b and d). Given that gahnite contains insignificant Fe^{3+} (Tab. 2), this most likely reflects the fact that the Fe^{2+} content of högbomite was underestimated in the calculation of structural formula after ZAKREWSKI (1977). The extreme case, in which all Fe is assumed to be ferrous in högbomite, is shown in figures 6 c and e. As expected, this results in regression lines intersecting the y-axis at positive values (dashed lines), providing support that Fe^{2+} is overestimated in högbomite. Although it is clear that direct determination of the Fe^{3+}/Fe^{2+} ratio in högbomite is a prerequisite for deriving precise partitioning data with other phases, the present results for low-grade rocks are quite useful for testing the temperature dependance of the Fe–Zn and Fe–Mg partitioning between högbomite and spinel.

A considerable amount of data have been reported in the literature on the Fe–Zn–Mg partioning between högbomite and spinel in amphibolite to granulite facies rocks. A selection, including only högbomite with > 2.0 wt% ZnO, is compared with the Samos data in figure 7. For reasons discussed above, it was decided to use total iron in the partitioning diagrams, resulting in maximum K_D values as högbomite generally appears

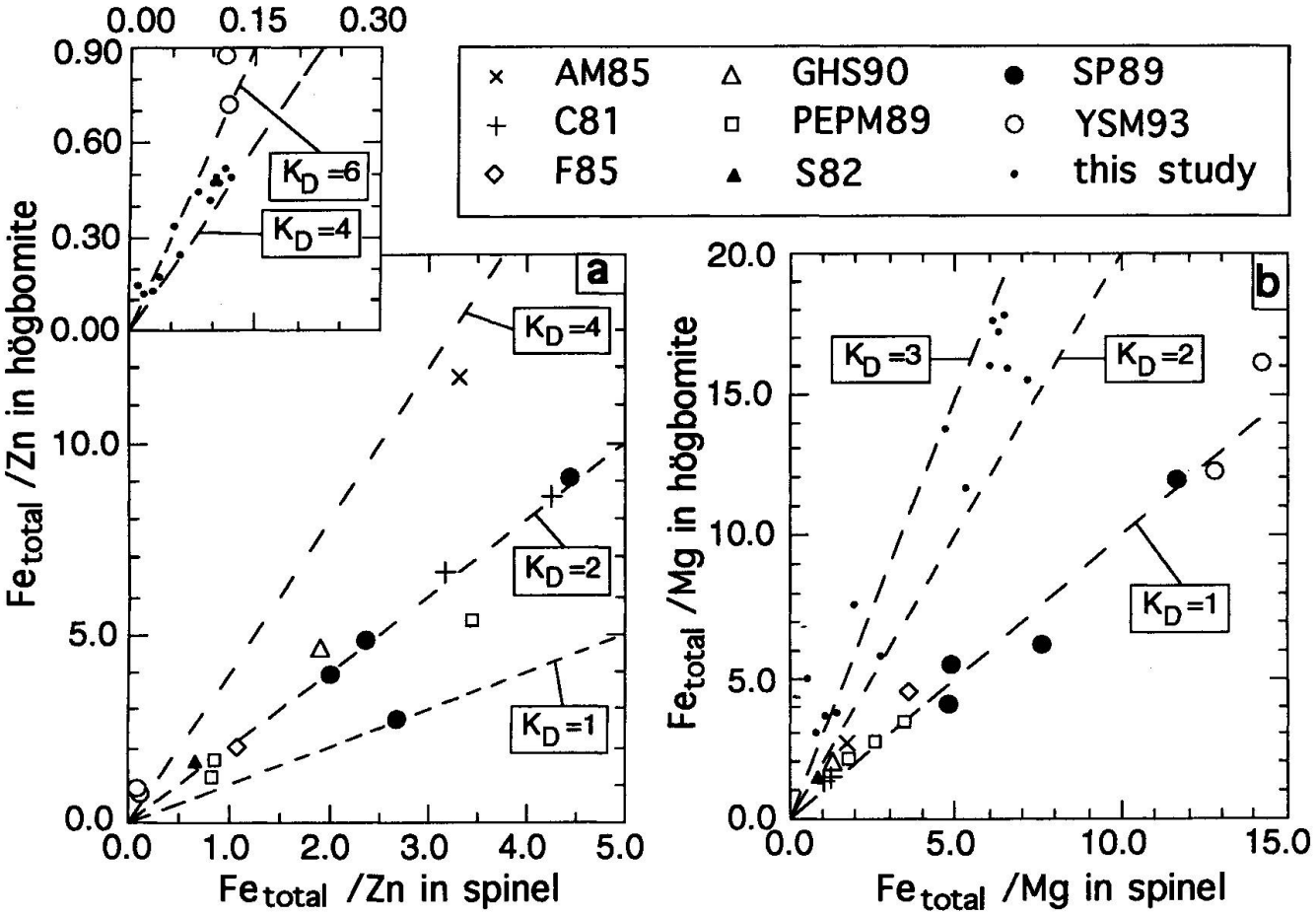

Fig. 7 Comparison of Fe_{tot}–Zn (a) and Fe_{tot}–Mg (b) partitioning between spinel and högbomite in Samos diasporites with that in higher grade rocks. Inset is enlargement of lower left corner of diagram (a). K_D lines are for reference only. Sources of plotted data: AM85, ANGUS and MIDDLETON, 1985; C81, COOLEN, 1981; F85, FEENSTRA, 1985; GHS90, GREW et al., 1990; PEPM89, PETERSEN et al., 1989; S82, SPRY, 1982; SP89, SPRY and PETERSEN, 1989; YSM93, YALÇIN et al., 1993.

to have higher Fe^{3+}/Fe^{2+} than the associated spinel (e.g., PETERSEN et al., 1989; VISSER et al., 1992; references given in Fig. 7). Figure 7 shows that Fe–Zn and Fe–Mg fractionation between högbomite and spinel is significantly stronger in the low-grade Samos diasporites than in the higher grade rocks. Whereas the distribution coefficient $K_D^{Ftot\text{-}Zn}{}_{ho\text{-}sp} = [(Fe_{tot}/Zn)ho/(Fe_{tot}/Zn)sp]$ falls in the range 4–6 for the Samos rocks, this K_D is chiefly around 2 for the amphibolite and granulite facies rocks. Similarly, $K_D^{Ftot\text{-}Mg}{}_{ho\text{-}sp} = [(Fe_{tot}/Mg)ho/ (Fe_{tot}/Mg)sp]$ falls in the range 2–3 for the Samos rocks and is around one in the high-grade equivalents (see also PETERSEN et al., 1989). The data for coexisting högbomite and gahnite in the Menderes metabauxites (YALÇIN et al., 1993), i.e. from comparable rocks only slightly higher in grade than the Samos ones, plot in line with Samos in figure 7a but follow the trend for high-grade rocks in figure 7b. The latter could relate, however, to the very minor and somewhat fluctuating MgO contents of the Menderes minerals, introducing large uncertainties in the plotted Fe_{tot}/Mg ratios. Although the element distribution between högbomite and spinel depicted in figure 7 may be obscured by "disregarding" ferric iron (particularly in högbomite) as well as any compositional dependence of K_D (the Samos högbomite and spinel are abnormally rich in Zn compared to most other data), the observed pattern provides support that it may have geothermometric potential.

Petrogenetic evolution

The (semi)pelitic and basic rock compositions of the Vourliotis unit (Fig. 1) show clear mineralogical evidence that they have been affected by an early high-P and later medium-P metamorphic event (CHEN, 1992: FEENSTRA and PETRAKAKIS, in prep.). For the intercalated diasporites this will imply a similar polymetamorphic P-T-t evolution. Texturally, Zn-staurolite and chloritoid are early phases, supporting an origin during the high-P metamorphism. Gahnite played a complex role in the petrogenesis of the studied rocks. As indicated by corroded gahnite inclusions in Zn-staurolite of the Samos (and Naxos) metabauxites (FEENSTRA and OCKENGA, in prep.), it was an early mineral and possibly the main Zn-providing phase in the Zn-staurolite-forming reaction. On the other hand, a second generation of small blue-coloured gahnite grains locally developed by partial breakdown of staurolite during the medium-P overprint. In chloritoid-bearing samples, the first-type gahnite is in textural equilibrium with chloritoid, suggesting that gahnite-chloritoid was a stable assemblage during both the high- and medium-P events. The extreme Zn-rich compositions measured in cores of large first-generation gahnites may represent relics of the high-P event. In the staurolite-bearing samples, the marginal parts of the first-type grains match in composition the second-type (homogeneous) gahnite grains, suggesting that the first-generation has marginally equilibrated during the medium-P event.

THE ZINCOHÖGBOMITE-FORMING REACTION

Textural observations generally indicate that zincohögbomite crystallized during the medium-P metamorphism. It developed at the expense of both the first and second generation gahnite. In staurolite-bearing samples, högbomite formation was coeval with, or slightly later than the the partial replacement of Zn-staurolite by second generation spinel, white Na–K–Ca micas and rare Ni-rich chlorite. In the other samples, a spatial relationship between högbomite and white micas is also common.

Rutile, occurring in minor amounts in all samples (occasionally in the högbomite-spinel intergrowths) may largely have provided the titanium contained in högbomite. Hematite that is strongly altered to Fe-hydroxides (containing < 1.5 wt% TiO_2) is present in traces in most samples (Tab. 1). It is likely that the primary hematite was more titaniferous, like in sample SA22A32 containing "fresh" Ti-hematite with 6.2–6.8 wt% TiO_2 (11–13 mole% ilmenite in solid solution). In the latter sample, Ti-hematite is a major phase, so that here hematite may have supplied significant Ti (and Fe) for the growth of högbomite.

The close association of zincohögbomite with gahnite in the Samos samples indicates a similar (but more complicated) reaction as proposed by YALÇIN et al. (1993) for the formation of zincian högbomite in the Menderes metabauxites. They observed that minor gahnite, coexisting with Ti-hematite and rutile, is common in Menderes diasporites metamorphosed at T = 360–430 ° C and P = ≈ 5 kb. With increasing grade, the Menderes gahnite reacts to zincian högbomite, leading to the disappearance of gahnite at emery grades (T = 430–500 ° C). YALÇIN et al. (1993) proposed that the formation of högbomite, taking place from temperatures of ≈ 400 °C onwards, can be approximated by the following reaction in the subsystem Fe–Zn–Ti–Al–H–O:

gahnite + diaspore + Ti-hematite + rutile
= högbomite + H_2O + O_2 (a)

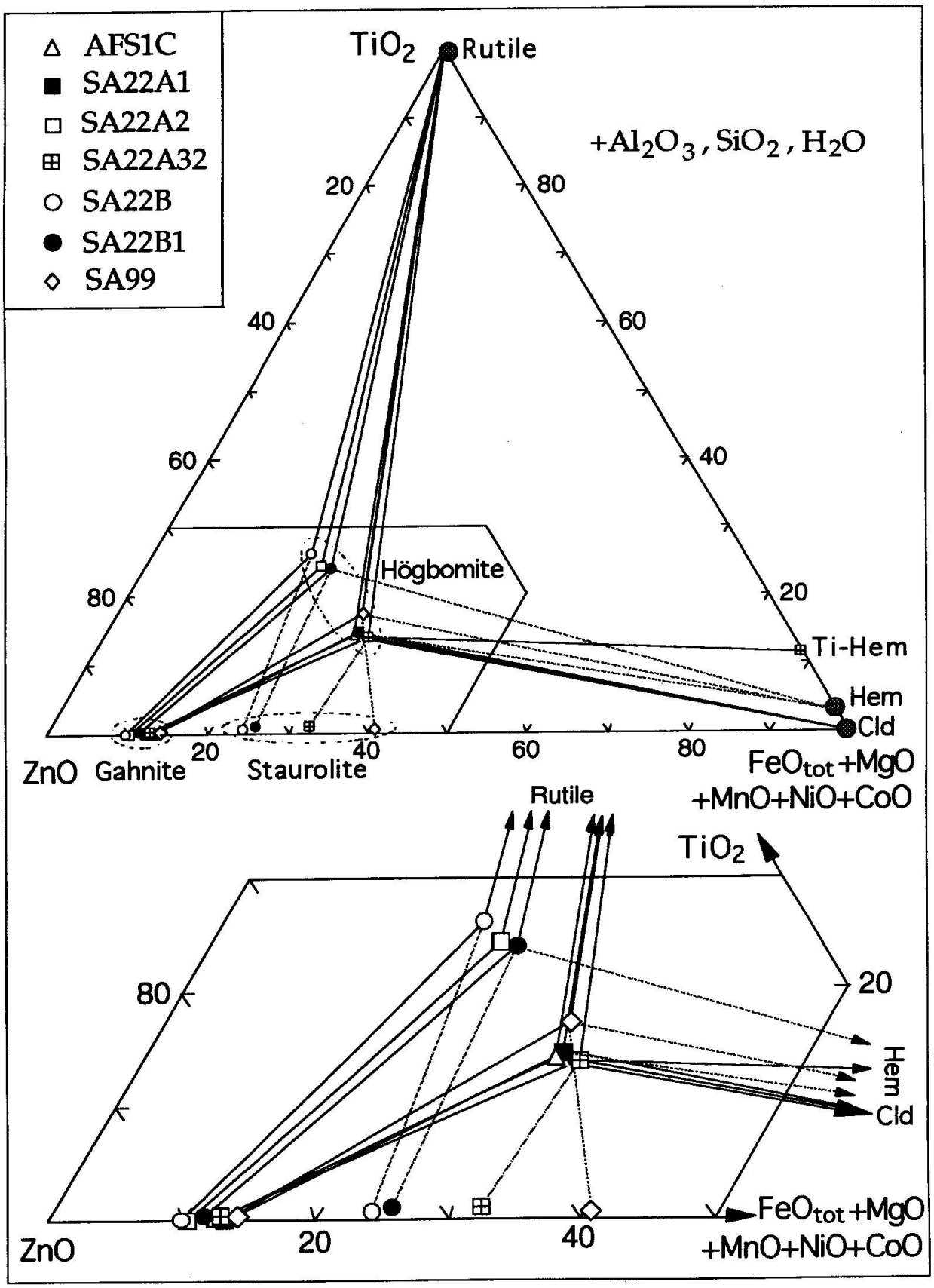

Fig. 8 Schematic ZnO–(FeO_{tot} + MgO + MnO + NiO + CoO)–TiO_2 diagram depicting phase relations pertinent to the formation of zincohögbomite. Lower diagram is enlargement of ZnO corner of upper diagram. For clarity only tie-lines towards zincohögbomite are shown. Dashed tie-lines towards Zn-staurolite and hematite indicate that it is uncertain whether högbomite is in equilibrium with these phases (see text).

In essence, textural evidence (Fig. 2) and chemical data (i.e. högbomite is systematically higher in Fe/Zn and Fe/Mg than gahnite; see Figs 3, 6 and 8) support reaction (a) in the Samos diasporites. The actual reaction, however, was more complex and partly different, because the Samos rocks are very poor in Fe and contain significant Ni and Co. Futhermore, the role of associated chloritoid and/or staurolite should also be considered.

Whereas Ti-hematite is an abundant (excess) phase in the main mass of the Menderes and Samos metabauxites, the studied samples typically contain only traces of (altered) Ti-hematite (except SA22A32) and two samples are devoid of hematite (Tab. 1). Contrary to a normal metabauxitic composition, where gahnite will determine the quantity of högbomite formed by reaction (a) (see YALÇIN et al., 1993), Ti-hematite may have played this role in the present samples. Alternatively, it may be argued that the Samos samples (except SA22A32) are not truly saturated with Ti-hematite, so that iron contained in högbomite has been derived from other phases. The schematic phase diagram of figure 8 allows the formation of högbomite from gahnite + rutile + chloritoid. In rocks, in which chloritoid dominates modally over högbomite, such a reaction may be continuous, leading to Mg (Mn) enrichment in chloritoid, coupled with minor formation of margarite (the Ca of which is supplied by calcite). The continuous reaction, which is supported by EMP data and textures showing (minor) marginal replacement of chloritoid by submicroscopic aggregates of white K–Na–Ca micas, can be approximated as follows:

gahnite + rutile + Fe-rich chloritoid + calcite
= högbomite + Fe-poorer chloritoid
+ margarite + H_2O + CO_2 (b)

Figure 8 shows that formation of högbomite from gahnite + rutile + staurolite is possible in sample SA99. In the other three staurolite-bearing rocks (SA22A32, 22B, 22B1), staurolite is slightly higher in X_{Zn} than högbomite, so that formation of högbomite from staurolite + rutile + Ti-hematite/chloritoid would be possible. As högbomite has never been seen in contact with staurolite and only sparsely occurs in the vicinity of staurolite, it seems unlikely that (partial) breakdown of Zn-staurolite was crucial for högbomite growth, the more so as högbomite is not restricted to staurolite-bearing samples (Tab. 1). Overall textural evidence and element partioning between högbomite and staurolite (cf. Fig. 8) even suggest that högbomite is partly out of equilibrium with staurolite in the studied samples.

In summary, textural and chemical data indicate that zincohögbomite formed primarily from gahnite, rutile and Ti-hematite/chloritoid. Diaspore, which is present in excess in all samples, may have participated in the reaction, and, in case chloritoid was a reactant, minor margarite (not shown in Fig. 8) may have formed concurrently with zincohögbomite [reaction (b)]. The precise zincohögbomite-forming reaction is, however, difficult to quantify, because of the complexity of the rock system, requiring the components Si, Mg, Ni, Co, Ca and C in addition to those for model reaction (a) in the Fe–Zn–Ti–Al–H–O system.

CONDITIONS OF ZINCOHÖGBOMITE FORMATION

Unfortunately, experimental data on the stability of högbomite and its phase relations are lacking. However, the associated minerals provide useful information on the physical conditions of högbomite growth. Phase relations in the Al_2O_3–SiO_2–H_2O system are important P-T monitors for the metamorphism of bauxites. Figure 9a shows the reaction relations between diaspore, corundum, quartz, kaolinite, pyrophyllite and Al-silicate. The diagrams of figures 9 a and b were calculated with the program MacPTAX (University of Berne, 1991) using GEØ-CALC software (BERMAN et al., 1987; BROWN et al., 1988). An updated version (BERMAN and ARANOVICH, 1996) of the database of BERMAN (1988) was used in the thermodynamic computations.

As zincohögbomite coexists with diaspore and not with corundum, the diaspore-corundum dehydration reaction gives a distinct upper temperature limit for högbomite growth (Fig. 9a). The phyllosilicates kaolinite and pyrophyllite are important P-T indicators; only minor amounts of kaolinite have been detected by EMP in white mica aggregates of samples SA22A1 and 22A32 (Tab. 1). If the kaolinite is truly part of the paragenesis accompanying högbomite, which is a matter of debate because kaolinite readily forms during weathering and alteration of rocks (MURRAY, 1988), then maximum temperatures for högbomite formation would be around 320 °C. Kyanite + pyrophyllite + quartz occurs in chloritoid-paragonite-muscovite bearing metaquartzitic rocks of the Vourliotis unit (CHEN, 1992: FEENSTRA and PETRAKAKIS, in prep.). This assemblage points to temperatures of 400–430 °C under conditions of $P_{tot} = P_{H_2O}$ (Fig. 9a).

Textures suggest the stable coexistence of högbomite with K–Na–Ca micas, which are common in the vicinity of gahnite-högbomite grains. Mus-

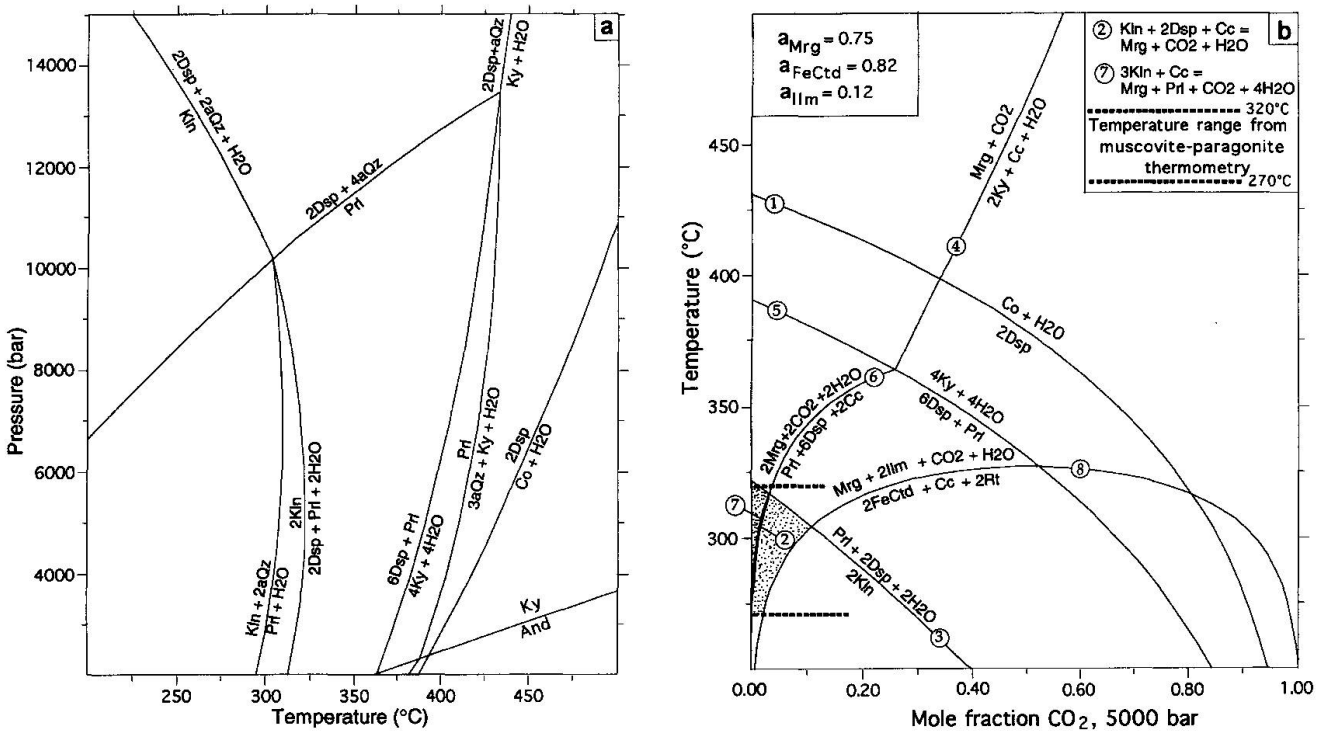

Fig. 9 (a) P_{H_2O}-T diagram for the Al_2O_3–SiO_2–H_2O system showing phase relations between diaspore (Dsp), corundum (Co), quartz (aQz), kyanite (Ky), andalusite (And), kaolinite (Kln) and pyrophyllite (Prl). Reactions in the andalusite field are not labeled. (b) T-X_{CO_2} diagram at P_{total} = 5000 bar showing reactions pertinent to the formation of margarite in metabauxitic compositions. Diagram was calculated for mineral compositions in sample SA22A32, assuming ideal mixing in margarite (X_{Ca} = 0.75), chloritoid (X^{2+}_{Fe} = 0.82) and Ti-hematite (X_{FeTiO_3} = 0.12) with all other phases considered to be pure. Temperatures obtained from muscovite-paragonite thermometry fall between the two dashed horizontal lines. Dotted field shows likely conditions for formation of Zn-högbomite, provided that kaolinite is a metamorphic phase (see text). All reactions were computed with the program MacPTAX (University of Berne, 1991) using GEØ-CALC software (BERMAN et al., 1987; BROWN et al., 1988) and the thermodynamic database of BERMAN and ARANOVICH (1996).

covite-paragonite solvus thermometry, using the calibration of BLENCOE et al. (1994) for quasibinary Na–K micas in medium-P (2–8 kbar) rocks, yields temperatures of 270–320 °C from white micas closely associated with zincohögbomite (FEENSTRA and OCKENGA, in prep.). This temperature range fits in with the occurrence of "metamorphic" kaolinite, provided that water activity was near unity in the Samos samples (Fig. 9). The presence of minor margarite in most samples, which may have formed by reactions (2) or (7) in the calcite-dominated diasporites, also fits in with temperatures around 300 °C under high water activity (Fig. 9b). An alternative equilibrium for the formation of margarite in the system FeO–TiO_2–CaO–Al_2O_3–SiO_2–H_2O–CO_2, calculated for mineral compositions measured in sample SA22A32, is also shown in figure 9b. As chloritoid and ilmenite-hematite were approximated as ideal solid solutions, the position of equilibrium (8) may be less certain than the positions of the reactions in the CaO–SiO_2–Al_2O_3–H_2O–CO_2 system. Nevertheless, equilibrium (8), which is supported by textural evidence in Aegean metabauxites (FEENSTRA, 1985 and 1996), allows formation of margarite from chloritoid + calcite at temperatures of ≈ 300 °C (at 5 kbar).

Pressure is poorly constrained by the mineralogy of the studied rocks. With increasing pressure, the margarite-producing reactions in figure 9b are generally displaced to higher temperatures and the stability field of margarite strongly decreases. At pressures ≥ 9 kbar, margarite is no longer stable and replaced by assemblages involving kyanite + zoisite, so that this is an upper P limit for the formation of zincohögbomite.

In summary, muscovite-paragonite thermometry and related kaolinite and margarite suggest that in the studied diasporite, zincohögbomite may have formed at temperaturs as low as ≈ 300 °C (at 5 kbar) under high a_{H_2O}. If the kaolinite is not part of the metamorphic paragenesis, then temperatures of högbomite growth may have been higher but were, in any case, within the diaspore stability field (< 430 °C at 5 kbar).

Discussion and concluding remarks

Gahnite and zincian högbomite are common minor to accessory phases in the greenschist-grade metabauxites of the Menderes Complex (YALÇIN, 1987; YALÇIN et al., 1993). Despite the study of several hundreds of thin sections, FEENSTRA (1985) did not detect these oxide minerals in the greenschist-grade metabauxites of Naxos or other Cycladic islands. The only exceptions are relictic gahnite inclusions within Zn-rich staurolite occurring in a Naxos metabauxite located slightly upgrade of the diaspore-corundum isograd (FEENSTRA and OCKENGA, in prep.). On Naxos, minor amounts of Fe–Zn–Mg spinel, and more rarely of Fe–Zn–Mg högbomite, first become widespread in the metabauxites at lower amphibolite-grade conditions. The higher temperature of formation is chemically reflected in the much higher Fe and Mg contents and lower Zn contents of the Naxos spinel and högbomite as compared with those of Samos and the Menderes Complex (cf. Fig. 7). Textural evidence indicates that, like the second-generation Samos gahnite, the Naxos spinel has largely developed by breakdown of Zn-bearing staurolite and that högbomite developed by partial replacement of Fe–Zn–Mg spinel (FEENSTRA, 1985).

The scarcity of högbomite in the greenschist-grade metabauxites of the Cyclades could be related to the fact that minor amounts of it may have been overlooked in thin section studies; optically, fine-grained högbomite somewhat resembles rutile, which is ubiquitious in the lower-grade Aegean metabauxites. For gahnite, typically forming isotropic octahedral grains, this possibility seems highly unlikely. The presence or absence of gahnite and högbomite thus most likely results from differences in chemical compostion and/or petrogenetic evolution between the Menderes, Samos and Central Cycladic metabauxites.

In general, metabauxites are highly heterogeneous rocks, complicating chemical comparison. YALÇIN (1987) showed that the overall chemical composition (including Zn content) of the Menderes metabauxites largely resembles that of the Naxos metabauxites. The average Zn content of the Menderes metabauxites is 421 ppm (range 40–1653; YALÇIN, 1987) and that of the Naxos metabauxites 429 ppm (range 60–1025; FEENSTRA and MAKSIMOVIĆ, 1985a). If the Menderes and Naxos metabauxites have comparable chemical compositions, then the occurrence of gahnite and zincian högbomite in the former could relate to a different metamorphic evolution. Whereas the Naxos metabauxites have been affected by an early Alpine high-P metamorphism followed by a medium-P overprint (FEENSTRA, 1985 and 1996), the Menderes metabauxites studied by YALÇIN (1987) only appear to have suffered Barrovian-type medium-P metamorphism. This different P-T-t path could indicate that incorporation of Zn in common metabauxitic minerals is favoured by increasing pressure, so that in the high-P metabauxites of the lower grade zones of Naxos, which only partially equilibrated during the medium-P overprint (FEENSTRA, 1996), all Zn could commonly be accommodated in minerals such as chloritoid and Fe-Ti-oxides, whereas in the Menderes metabauxites this was not always possible, resulting in additional trace amounts of gahnite and Zn-rich högbomite.

Geochemical data for the samples of the present study are not yet available but it is obvious that their composition is not representative for the bulk of the Samos and Aegean metabauxites. In fact, the samples are not true bauxites but mixtures of limestone and bauxite, as reflected in their high amounts of calcite (> 60% by volume). Chemically, they are highly enriched in Zn, Ni, Co, Y and REE and strongly depleted in Fe and Mg (FEENSTRA and OCKENGA, in prep.), so that the enriched elements, particularly Zn, can never be incorporated in the common metabauxitic minerals.

Although the partial replacement of staurolite and chloritoid by muscovite and paragonite suggests that alkalis have locally been introduced into the marginal parts of the studied diasporite lens by late water-rich fluids, the overall petrological evidence does not support a widespread metasomatic activity. Hence it is most likely that the Samos samples acquired their unusual bulk composition during the pre-metamorphic stage.

FEENSTRA and MAKSIMOVIĆ (1985b) studied vertical profiles across greenschist- to amphibolite-grade metabauxite lenses on Naxos and demonstrated that vertical trace element distribution patterns characteristic for karstbauxites formed in situ have survived metamorphism. These patterns typically involve syngenetic downward enrichment of Ni, Co, Zn, Mn, Cu, Pb, Y and REE (e.g., MAKSIMOVIĆ, 1978; MAKSIMOVIĆ and DE WEISSE, 1979). At the carbonate footwall of karstbauxite deposits, these elements may become enriched by factors of 10–100 relative to the bulk of the bauxite. A similar pre-metamorphic geochemical process may be envisaged to have created the unusual bulk compositions on Samos, because the Zn-, Ni- and Co-rich minerals typically occur at the lower contact between diasporite and marble. During subsequent metamorphism this then led to the local formation of Zn-dominated (Ni-Co-rich) staurolite, spinel and

högbomite at metamorphic temperatures much lower than typical for the occurrence of the Fe-dominated members.

Acknowledgements

I thank Urs K. Mäder (Bern) and Werner Schreyer (Bochum) for constructive reviews of the manuscript and Kostas Petrakakis (Vienna) for collaboration and helpful discussions on Samos geology. The study was supported by the "Fonds zur Förderung der wissenschaftlichen Forschung", Austria (projects P9583-GEO and P10821-GEO). Most EMP work was performed at the Mineralogical-Petrological Institute, University of Berne, using a CAMECA SX-50 supported by the "Schweizerischer Nationalfonds".

References

ANGUS, N.S. and MIDDLETON, R. (1985): Compositional variation in högbomites from north Connemara, Ireland. Min. Mag. 49, 649–654.

BERMAN, R.G. (1988): Internally-consistent thermodynamic data for minerals in the system Na_2O–K_2O–CaO–MgO–FeO–Fe_2O_3–Al_2O_3–SiO_2–TiO_2–H_2O–CO_2. J. of Petrology 29, 445–522.

BERMAN, R.G. and ARANOVICH, L.Y. (1996): Optimized standard state and solution properties of minerals: I. Model calibration for olivine, orthopyroxene, cordierite, garnet, and ilmenite in the system FeO–MgO–CaO–Al_2O_3–SiO_2–TiO_2. Contrib. Mineral. Petrol. 126, 1–24.

BERMAN, R.G., BROWN, T.H. and PERKINS, E.H. (1987): GEØ-CALC: Software for calculation and display of P-T-X phase diagrams. Am. Mineral. 72, 861–862.

BLENCOE, J.G., GUIDOTTI, C.V. and SASSI, F.P. (1994): The paragonite-muscovite solvus: II. Numerical geothermometers for natural, quasibinary paragonite-muscovite pairs. Geoch. et Cosmochim. Acta 58, 2277–2288.

BROWN, T.H, BERMAN, R.G. and PERKINS, E.H. (1988): GEØ-CALC: Software package for calculation of pressure-temperature-composition phase diagrams using an IBM or compatible personal computer. Comp. Geosci. 14, 279–289.

ČECH, F., RIEDER, M. and VRANA, S. (1976): Cobaltoan högbomite from Zambia. N. Jb. Miner. Mh. 1976, 525–531.

CHEN, G. (1992): Evolution of the high- and medium-pressure metamorphic rocks on the island of Samos, Greece. Ph. D. Thesis, University of Würzburg, 172 pp.

COOLEN, J.J.M.M.M. (1981): Högbomite and aluminium spinel from some metamorphic rocks and Fe–Ti ores. N. Jb. Miner. Mh. 1981, 374–384.

DÜRR, ST. (1975): Über Alter und geotektonische Stellung des Menderes-Kristallins/SW-Anatolien und seine Äquivalente in der mittleren Ägäis. Habil. Schrift, University of Marburg, 107 pp.

DÜRR, ST. (1986): Das Attisch-Kykladische Kristallin. In JACOBSHAGEN, V. (ed.): Geologie von Griechenland, 116–149. Gebrüder Borntraeger, Berlin.

FEENSTRA, A. (1985): Metamorphism of bauxites on Naxos, Greece. Ph. D. Thesis, University of Utrecht. Geologica Ultraiectina 39, 206 pp.

FEENSTRA, A. (1996): An EMP and TEM-AEM study of margarite, muscovite and paragonite in polymetamorphic metabauxites of Naxos (Cyclades, Greece) and the implications of fine-scale mica interlayering and multiple mica generations. J. of Petrology 37, 201–233.

FEENSTRA, A. and MAKSIMOVIĆ, Z. (1985a): Geochemistry of diaspore and corundum-bearing metabauxites from Naxos, Greece. Part I: Major and trace element chemistry, and geochemical evidence of a Jurassic stratigraphic age. In: FEENSTRA, A. Metamorphism of bauxites on Naxos, Greece. Ph. D. Thesis University of Utrecht, Geologica Ultraiectina 39, 137–173.

FEENSTRA, A. and MAKSIMOVIĆ, Z. (1985b): Geochemistry of diaspore and corundum-bearing metabauxites from Naxos, Greece. Part II: The existence of premetamorphic trace element patterns in amphibolite facies metabauxite lenses and their use as geochemical top and bottom indicators. In: FEENSTRA, A.: Metamorphism of bauxites on Naxos, Greece. Ph. D. Thesis University of Utrecht, Geologica Ultraiectina 39, 175–206.

FROST, B.R. (1991): Stability of oxide minerals in metamorphic rocks. In: LINDSLEY, D.H. (ed.): Oxide Minerals: petrologic and magnetic significance. Mineral. Soc. America, Rev. in Mineral. 25, 469–498.

GATEHOUSE, B.M. and GREY, I.E. (1982): The crystal structure of högbomite-8H. Am. Mineral. 67, 373–380.

GREW, E.S., ABRAHAM, K. and MEDENBACH, O. (1987): Ti-poor högbomite in kornerupine-cordierite-sillimanite rocks from Ellammankovilpatti, Tamil Nadu, India. Contrib. Mineral. Petrol. 95, 21–31.

GREW, E.S., HIROI, Y. and SHIRAISHI, K. (1990): Högbomite from the the Prince Olav Coast, east Antartica: An example of oxidation-exsolution of a complex magnetite solid solution? Am. Mineral. 75, 589–600.

KRETZ, R. (1983): Symbols for rock-forming minerals. Am. Mineral. 68, 277–279.

LAPPERENT DE, J. (1937): L'émeri de Samos. Tschermaks Min. Petrogr. Mitt. 49, 1–30.

MAKSIMOVIĆ, Z. (1978): Nickel in karstic environment: in bauxites and karstic nickel deposits. Bull. du B.R.G.M. (2) II, 173–183.

MAKSIMOVIĆ, Z. and DE WEISSE, G. (1979): Geochemical study of an overturned bauxite deposit in Les Codouls (S. France). Travaux ISCOBA 15, 109–120.

MCKIE, D. (1963): The högbomite polytypes. Min. Mag. 33, 563–580.

MPOSKOS, E. (1978): Diasporit- und Smirgelvorkommen der Insel Samos. Proc. 4th Int. Congress ISCOBA, Athens 1978, Vol. 2, 614–631.

MPOSKOS, E. and PERDIKATZIS, V. (1981): Die Paragonit-Chloritoid führenden Schiefer des südwestlichen Bereiches des Kerkis auf Samos (Griechenland). N. Jb. Miner. Abh. 142, 292–308.

MPOSKOS, E., SKARPELIS, N., PERDIKATZIS, V. and LIATI, A. (1990): Titanium-rich metagabbros from Samos, Aegean island (Greece). Proceedings Int. Earth Sci. Congress on Aegean Regions, Izmir Turkey, Vol. 1, 275–290.

MURRAY, H.H. (1988): Kaolin minerals: their genesis and occurrences. In: BAILEY, S.W. (ed.): Hydrous phyllosilicates (exlusive of micas). Min. Soc. of America, Rev. in Mineral. 19, 67–89.

OCKENGA, E. (1989): Zinkhögbomit aus Metabauxiten von Samos (Griechenland). Beiheft Eur. J. Mineral. 1, 140.

OCKENGA, E., YALÇIN, U., MEDENBACH, O. and SCHREY-

ER, W. (in prep.): Zincohögbomite-(8H), a new mineral in eastern Aegean metabauxites. Eur. J. Mineral.

OKRUSCH, M. and BRÖCKER, M. (1990): Eclogites associated with high-grade blueschists in the Cyclades archipelago, Greece: a review. Eur. J. Mineral. 2, 451–478.

OKRUSCH, M., RICHTER, P. and KATSIKATSOS, G. (1984): High-pressure rocks of Samos, Greece. In: DIXON, J.E. and ROBERTSON, A.H.F. (eds): The Geological Evolution of the Eastern Mediterranean. Geol. Soc. Spec. Publ. 17, 529–536. Blackwell, Oxford.

ÖNAY, T.S. (1949): Über die Smirgelgesteine Südwest-Anatoliens. Schweiz. Mineral. Petrogr. Mitt. 29, 357–491.

PAPANIKOLAOU, D.J. (1979): Unités tectoniques et phases de déformation dans l'île de Samos, Mer Egée, Grèce. Bull. Soc. géol. France 21, 745–752.

PETERSEN, E.U., ESSENE, E.J., PEACOR, D.R. and MARCOTTY, L.A. (1989): The occurrence of högbomite in high-grade metamorphic rocks. Contrib. Mineral. Petrol. 101, 350–360.

POUCHOU, J.L. and PICHOIR, F. (1985): "PAP" ϕ (ρZ) procedure for improved quantitative microanalysis. Microbeam Anal. 1985, 104–106.

RAMMLMAIR, D., MOGESSIE, A., PURTSCHELLER, F. and TESSADRI, R. (1988): Högbomite from the Vumba schist belt, Botswana. Am. Mineral. 73, 651–656.

SANDHAUS, D.J. and CRAIG, J.R. (1986): Gahnite in the metamorphosed stratiform massive sulfide deposits of the Mineral District, Virginia, U.S.A. Tschermaks Min. Petr. Mitt. 35, 77–98.

SCHLIESTEDT, M., ALTHERR. R. and MATTHEWS, A. (1987): Evolution of the Cycladic Crystalline Complex: petrology, isotope geochemistry and geochronology. In HELGESON, H.C. (ed.): Chemical transport in metasomatic processes. NATO ASI Series C 218. D. Reidel Publishing Company, Dordrecht, 389–428

SCHMETZER, K. and BERGER, A. (1990): Lamellar iron-free högbomite-24R from Tanzania. N. Jb. Miner. Mh. 1990, 401–412.

SPRY, P.G. (1982): An unusual gahnite-forming reaction, Geco base-metal deposit, Manitouwadge, Ontario. Can. Mineral. 20, 549–553.

SPRY, P.G. and PETERSEN, E.U. (1989): Zincian högbomite as an exploration guide to metamorphosed massive sulphide deposits. Min. Mag. 53, 263–269.

THEODOROPOLOUS, D. (1979): Geological Map of Greece 1:50'000, Samos Island. N.I.G.M.R, Athens.

VISSER, D., THYSSEN, P.H.M. and SCHUMACHER, J.C. (1992): Högbomite in sapphirine-bearing rocks from the Bamble Sector, south Norway. Min. Mag. 56, 343–351.

WILSON, A.F. (1977): A zincian högbomite and some other högbomites from the Strangways Range, Central Australia. Min. Mag. 41, 337–344.

WYBRANS, J.R. and MCDOUGALL, I. (1988): Metamorphic evolution of the Attic Cycladic Metamorphic Belt on Naxos (Cyclades, Greece) utilizing $^{40}Ar/^{39}Ar$ age spectrum measurements. J. met. Geology 6, 571–594.

YALÇIN, U. (1987): Petrologie und Geochemie der Metabauxite SW-Anatoliens. Ph. D. Thesis, Ruhr University, Bochum, 146 pp.

YALÇIN, U., SCHREYER, W. and MEDENBACH, O. (1993): Zn-rich högbomite formed from gahnite in the metabauxites of the Menderes Massif, SW Turkey. Contrib. Mineral. Petrol. 113, 314–324.

ZAKRZEWSKI, M.A. (1977): Högbomite from the Fe–Ti deposit of Liganga (Tanzania). N. Jb. Miner. Mh. 1977, 373–380.

Manuscript received April 15, 1996; revised manuscript accepted November 29, 1996.